Max-Plank-Institute for Solid State Research

NEW METHODS FOR INCREASING ACCURACY OF *IN-SITU* POWDER DIFFRACTION

APD-IV
NIST
Gaithersburg, April 22-25, 2013

Robert E. Dinnebier
Martin Etter
Oksana Magdysyuk
Melanie Müller
Tomče Runčevski

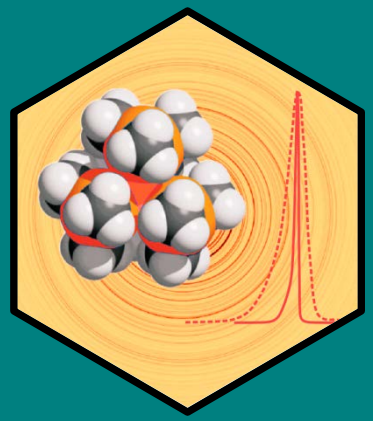

OUTLINE

- The method of *in-situ* powder diffraction
- „bottle necks“ and possible solutions
- State of the art examples:
  - Monitoring of mechanochemical milling reactions
  - Gas adsorption in large pore MOF’s
  - Advances in MEM analysis
- Conclusions

THE METHOD OF CHOICE: TIME RESOLVED '*IN SITU*' POWDER DIFFRACTION

Phase transitions

- ‚Polymorph screening'
- Phase transitions of different order
- Reversibility of phase transitions (hysteresis, strain-order parameter coupling)

Chemical reactions

- solid/solid, liquid/liquid, solid/gaseous etc.
- Influence of external conditions (pressure, temperature, stress, Electric/magnetic field, Light, mechanical power, etc.)

Physical effects

- thermal expansion (change of bond lengths, cell volume, cell axes etc.)
- Compressibility (bulk modulus)
- structural changes

CRYSTAL STRUCTURE FROM '*IN SITU*' POWDER DIFFRACTION: THE BEGINNING…

An early ‚in-situ' powder xray diffraction experiment on the structure of α-N_2

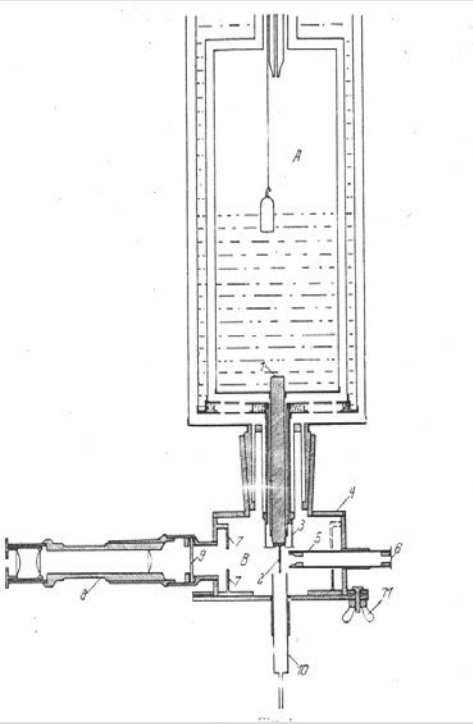

Schematic drawing of the used cryo-camera

Fig. 2.

Debye-Scherrer film of α-N_2 at 34K

Exposure time: 18h

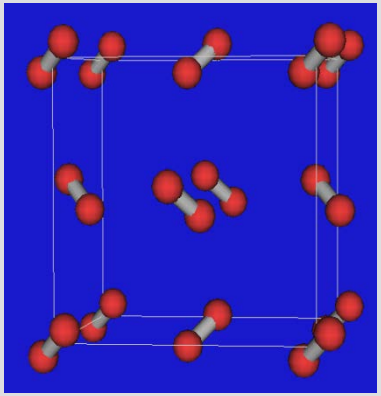

α-N_2 *Pa*-3

VEGARD, L. (1929). *Z. Phys.* 58, 497-501.

THE BOTTLE NECKS

- Scanning Speed

- Instrumental Resolution

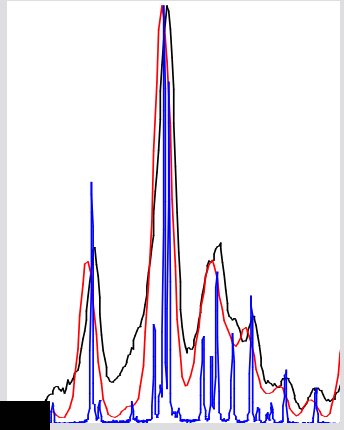

- Data Reduction Software

WHY BETTER RESOLUTION…

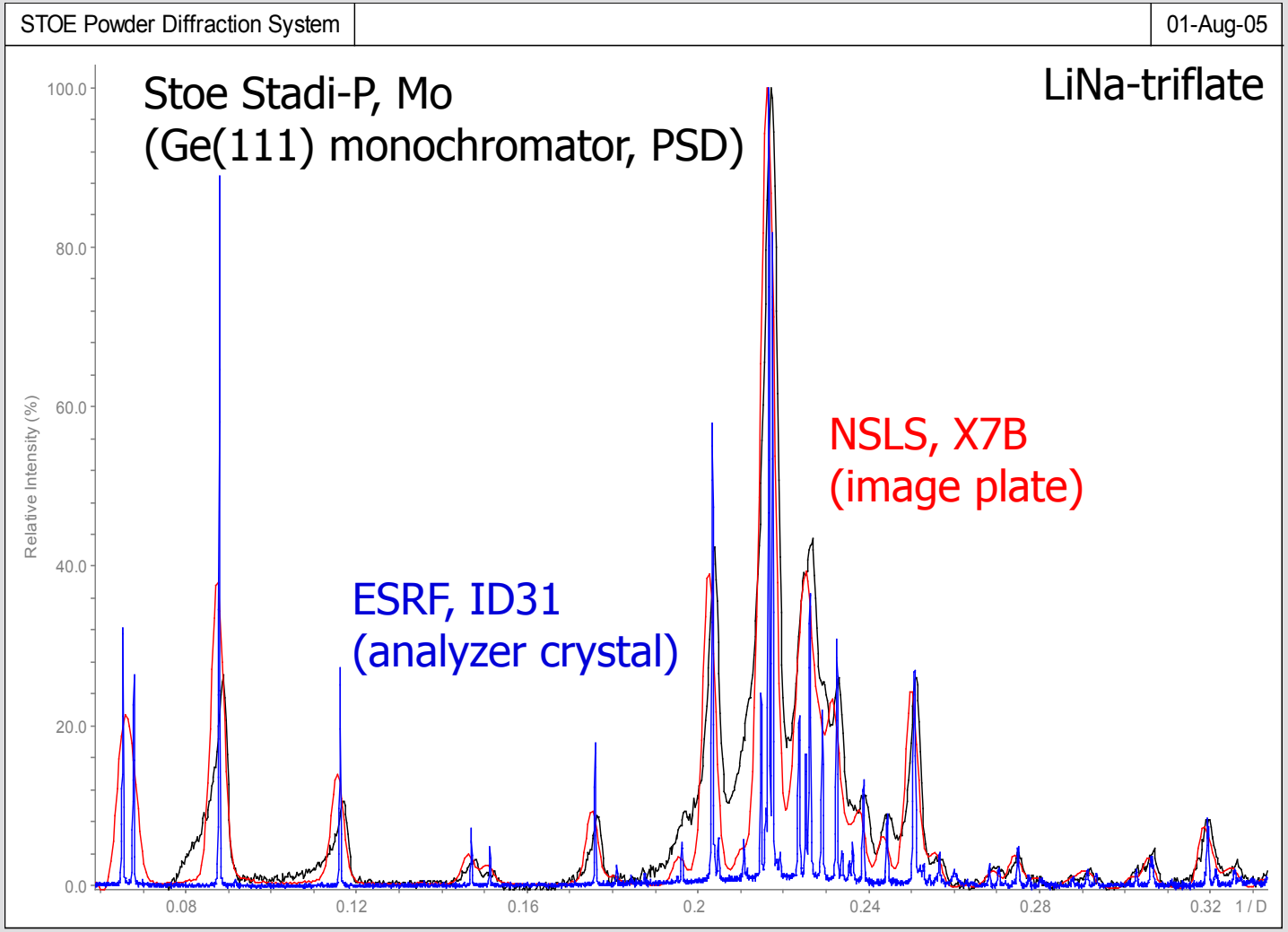

WHY HIGHER SPEED

5 minutes/scan

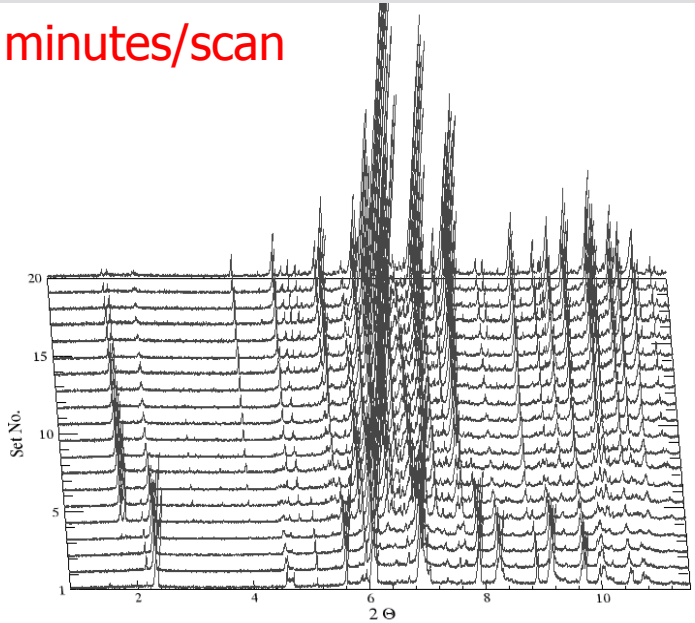

1 minute/scan

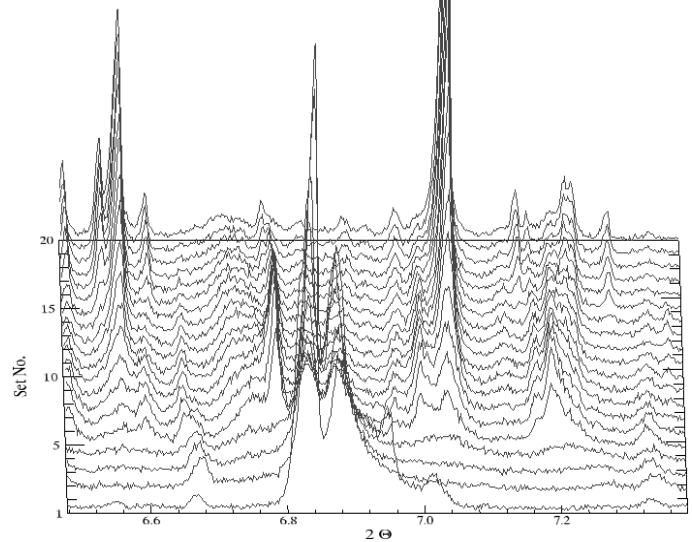

30 seconds/scan

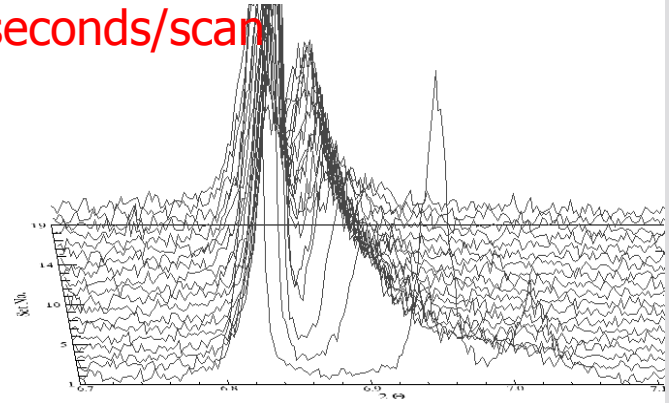

Radiation induced phase transition of Rubidium triflate measured at ID31, ESRF, July, 2005

WHY BETTER SOFTWARE

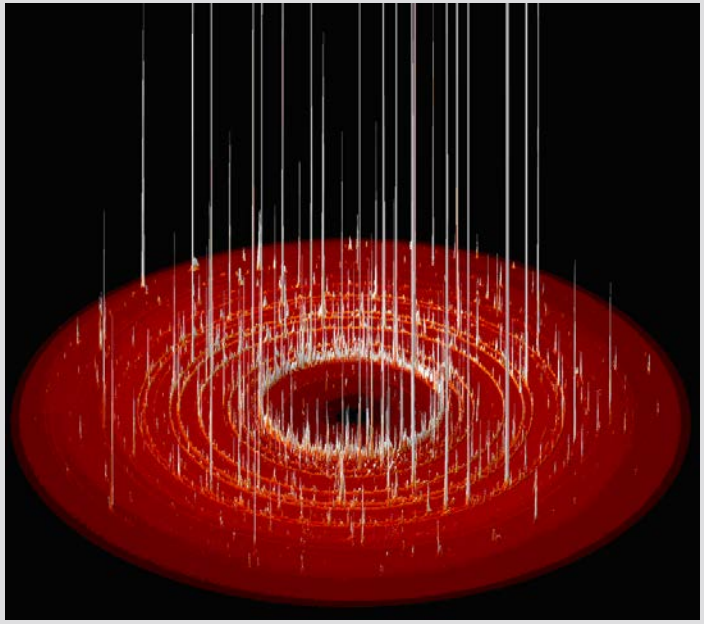

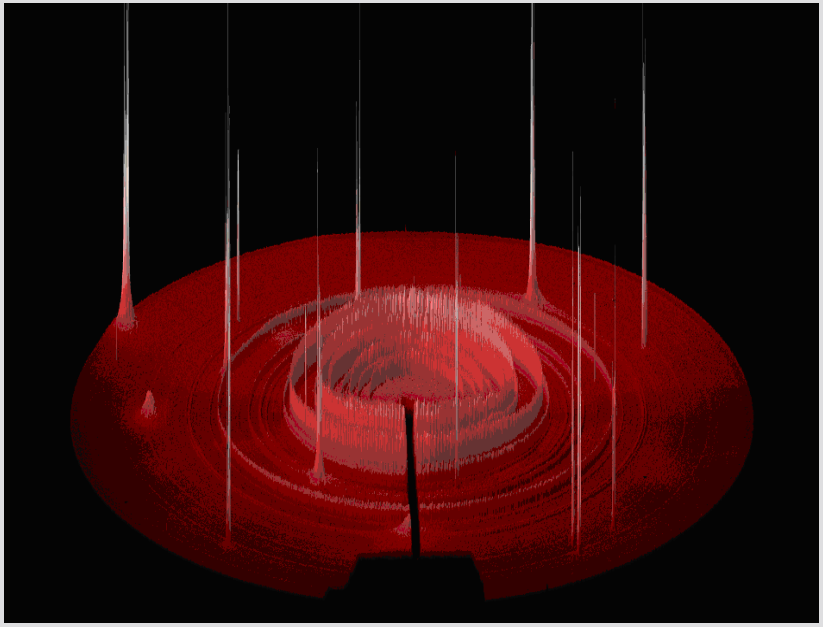

Rendered images of a high pressure powder diffraction data set (left) and a high temperature powder diffraction data set (right) collected by a 2D-image plate detector.

The white spikes are high intensity peaks originating from larger grains within a fine grained matrix (left) or reflections of the high temperature sapphire capillary (right).

SOLUTION OF THE SPEED/RESOLUTION PROBLEM: HIGH RESOLUTION PSD'S

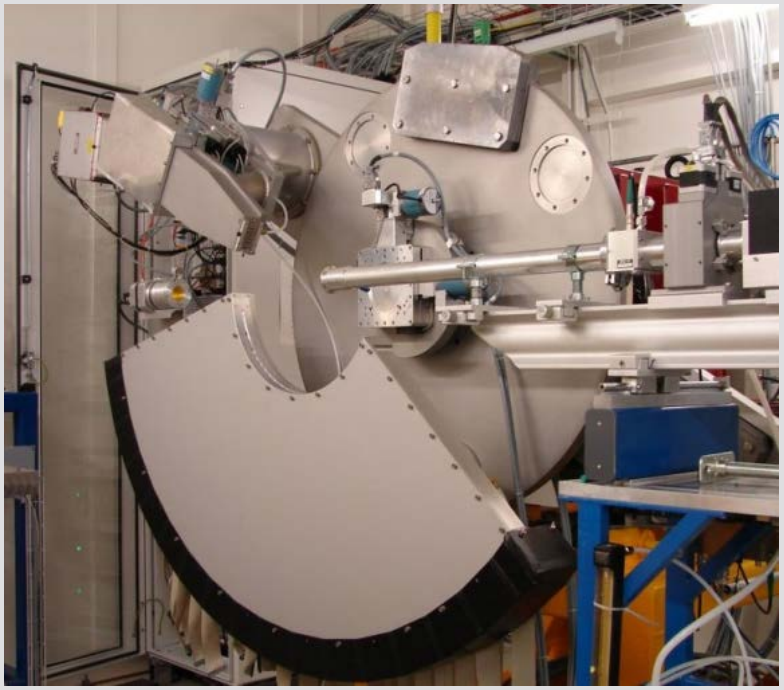

The 30720-element Mythen II strip detector, covering 120° at the SLS

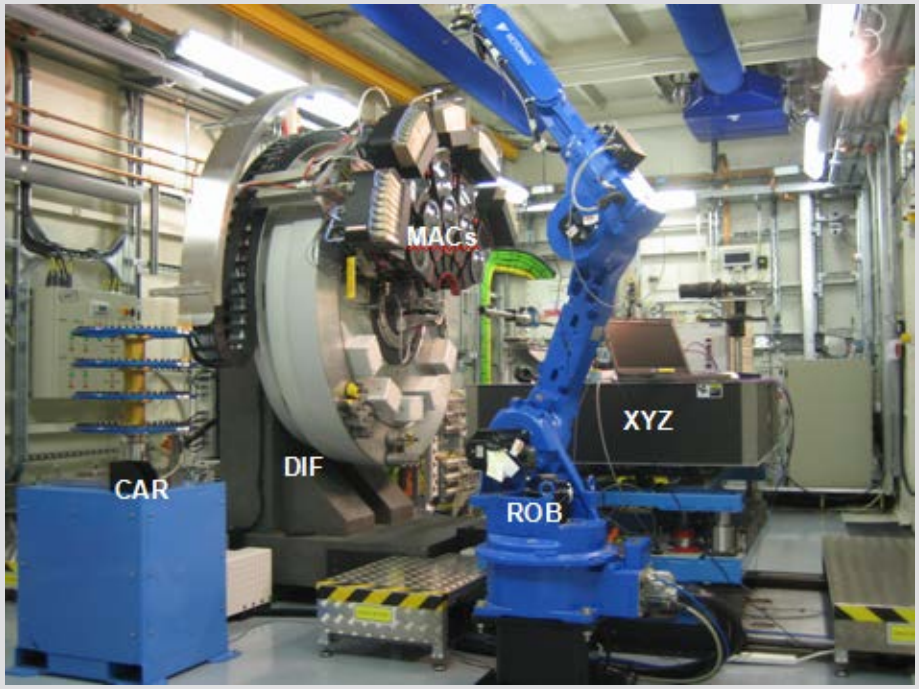

5* with 9 Si(111) analyzing crystals at I11, Diamond

IMPROVING DATA REDUCTION BY THROWING AWAY INFORMATION

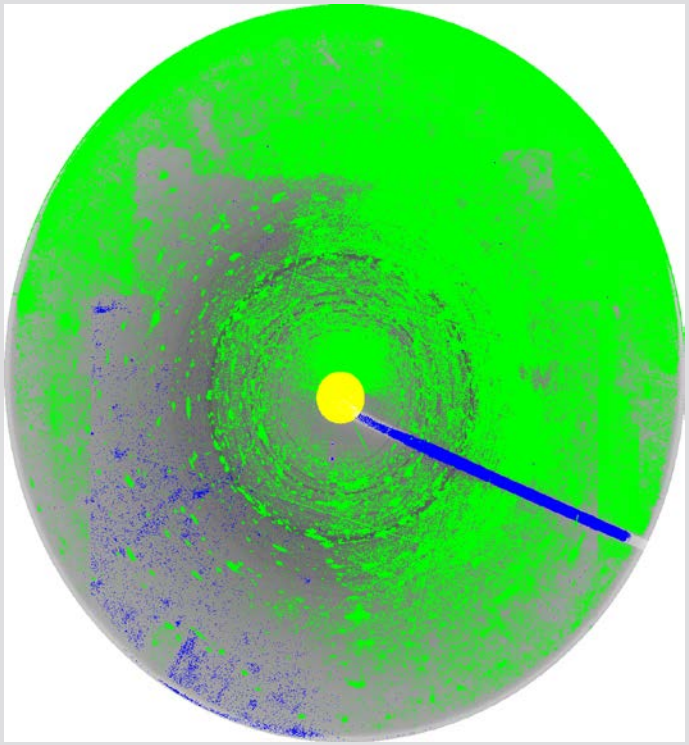

Green mask: top 48%.
Blue mask: bottom 2%
Yellow mask: beam stop
Grey region: used for integration

The effect of fractile filtering on the diffraction image is shown:

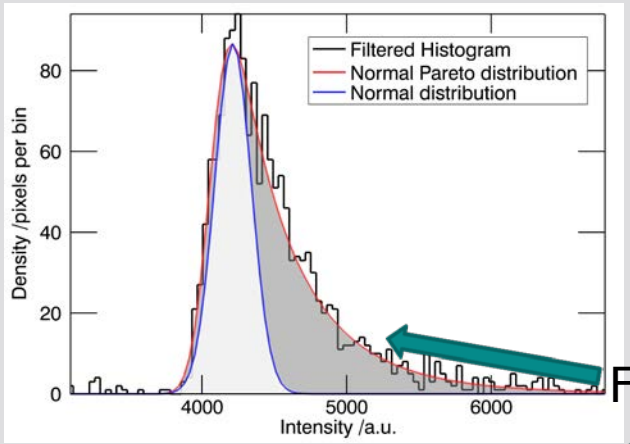

Filtered part

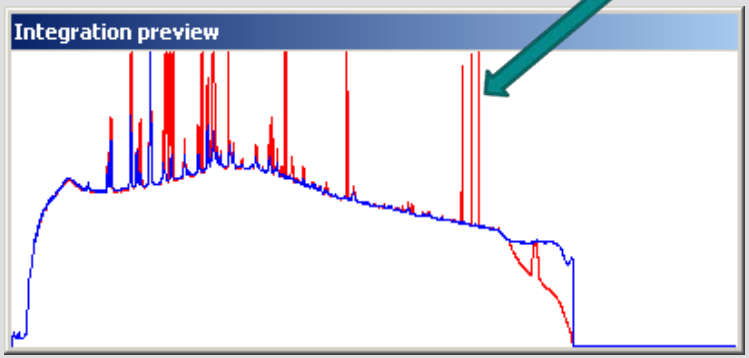

BENEFIT FOR DETECTING PHASE TRANSITIONS

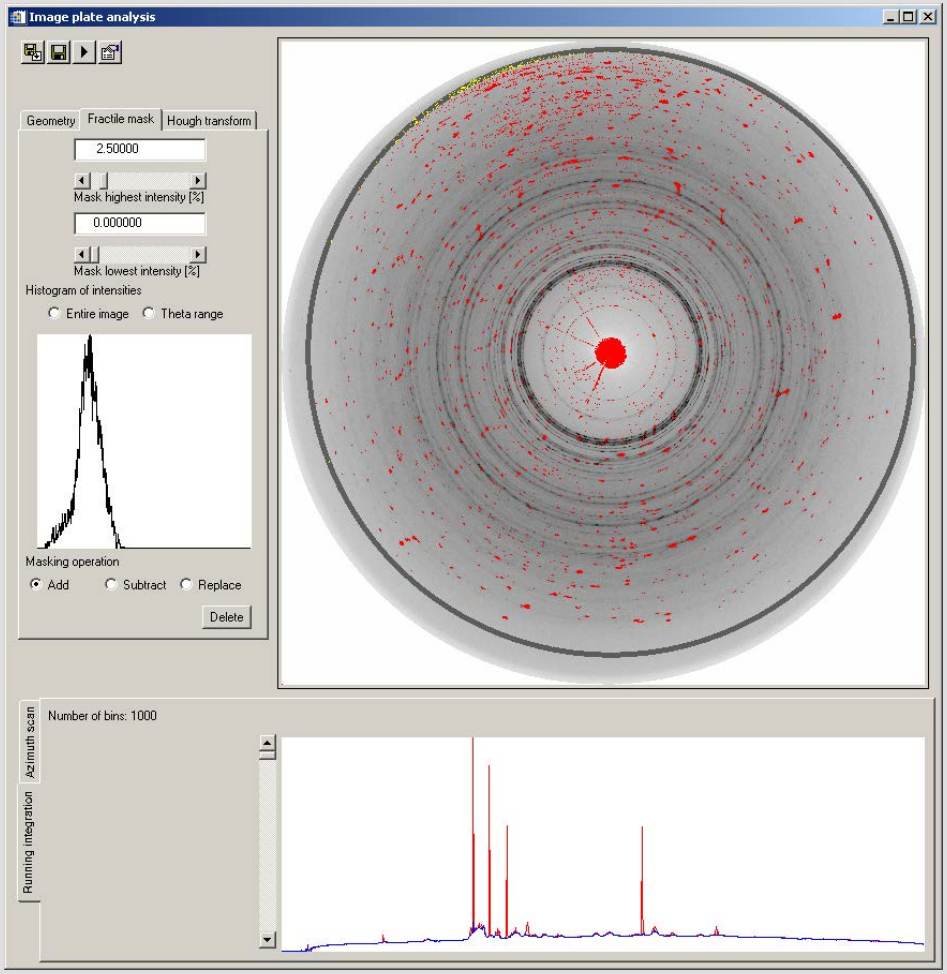

$FeSb_2O_4$ at 53 kbar

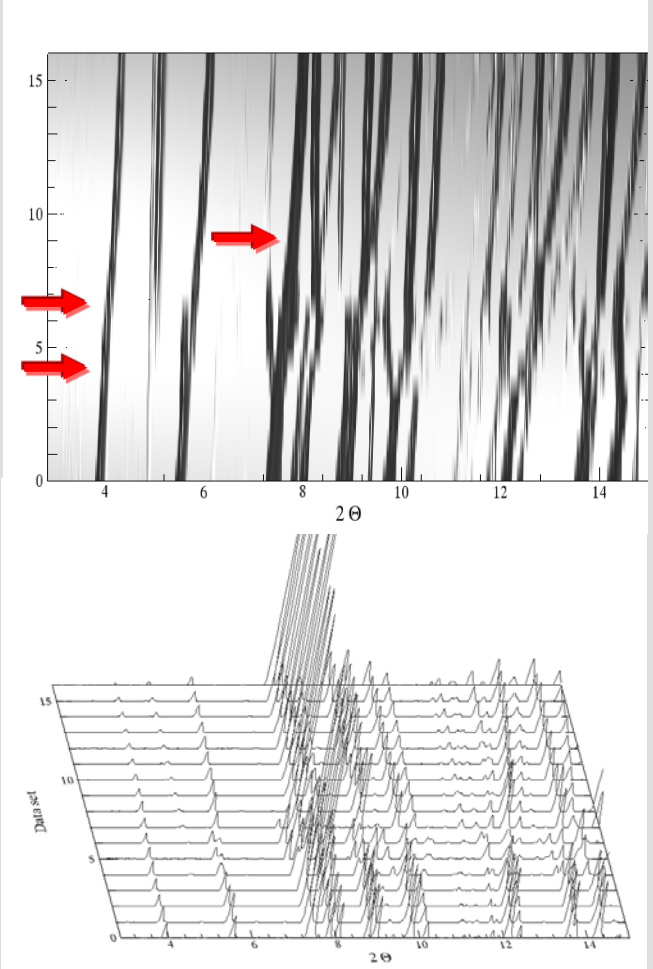

Final integrated powder patterns

REAL-TIME AND IN SITU MONITORING OF MECHANOCHEMICAL MILLING REACTIONS

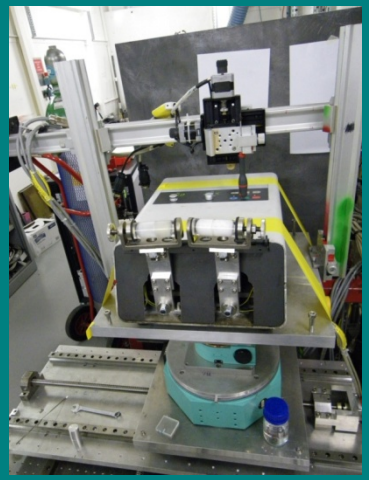

Tomislav Friščić, Ivan Halasz, Patrick J. Beldon, Ana M. Belenguer, Frank Adams, Simon A.J. Kimber, Veijo Honkimäki, Robert E. Dinnebier

2013, Nature Chemistry 5, 66–73.

MECHANOCHEMISTRY: DIFFERENT WAYS OF INTRODUCING ENERGY INTO A REACTION:

Heat

Radiation/electricity

Grinding (mechanical force)

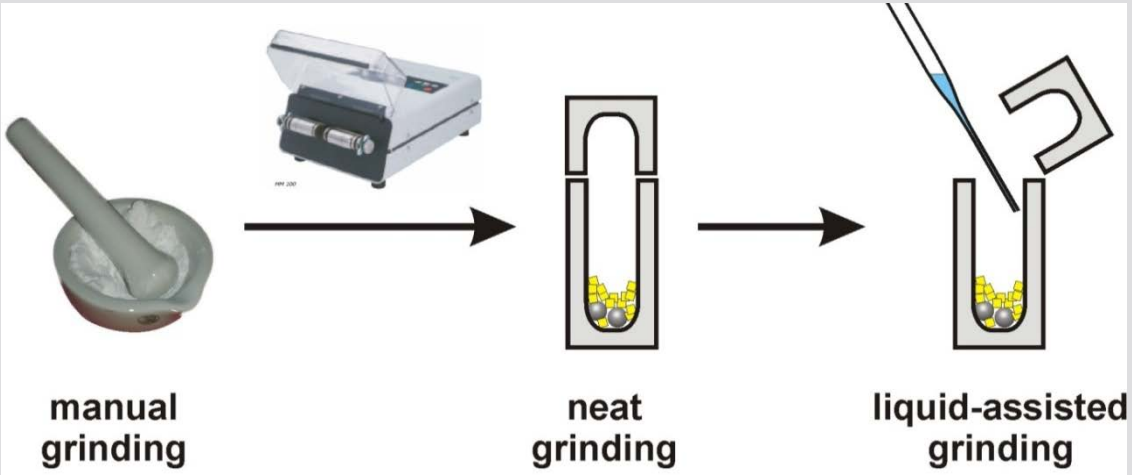

James, Collier, Parkin, Hyatt, Braga, Maini, Jones, Bölm, Krebs, Mack, Waddell, Shearhouse, Orpen, Adams, Friščić, Steed, Harris "Mechanochemistry: new and cleaner synthesis" Chem. Soc. Rev. ***2012****, 41,* 413-447.

METAL-ORGANIC FRAMEWORKS (MOFS) - ARCHETYPAL MODERN MATERIALS

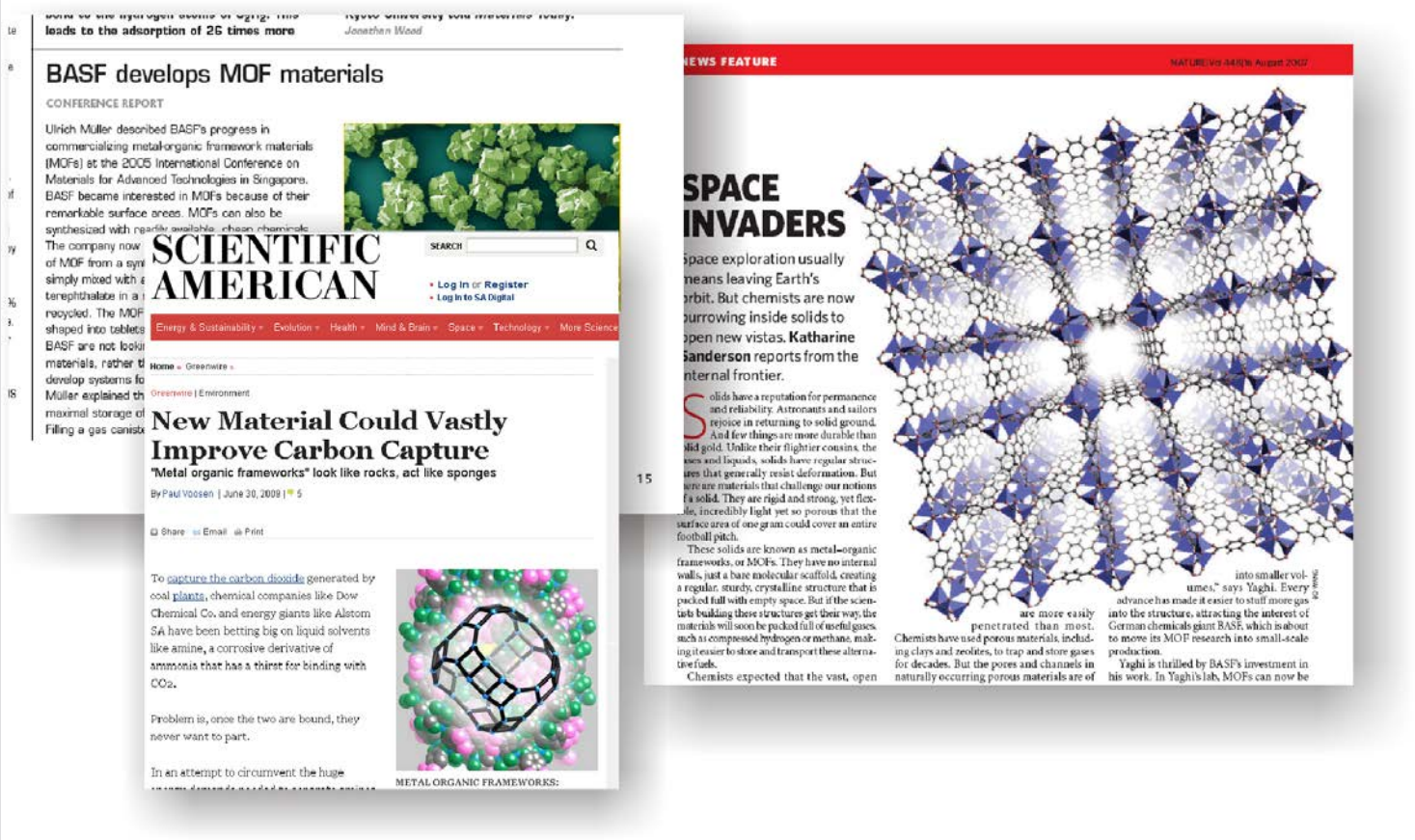

BASF develops MOF materials

CONFERENCE REPORT

Ulrich Müller described BASF's progress in commercializing metal-organic framework materials (MOFs) at the 2005 International Conference on Materials for Advanced Technologies in Singapore. BASF became interested in MOFs because of their remarkable surface areas. MOFs can also be synthesized with readily available, cheap chemicals

SCIENTIFIC AMERICAN

Energy & Sustainability | Evolution | Health | Mind & Brain | Space | Technology | More Science

Greenwire | Environment

New Material Could Vastly Improve Carbon Capture

"Metal organic frameworks" look like rocks, act like sponges

By Paul Voosen | June 30, 2009

To capture the carbon dioxide generated by coal plants, chemical companies like Dow Chemical Co. and energy giants like Alstom SA have been betting big on liquid solvents like amine, a corrosive derivative of ammonia that has a thirst for binding with CO_2.

Problem is, once the two are bound, they never want to part.

In an attempt to circumvent the huge

METAL ORGANIC FRAMEWORKS:

NEWS FEATURE

NATURE|Vol 448|9 August 2007

SPACE INVADERS

Space exploration usually means leaving Earth's orbit. But chemists are now burrowing inside solids to open new vistas. Katharine Sanderson reports from the internal frontier.

Solids have a reputation for permanence and reliability. Astronauts and sailors rejoice in returning to solid ground. And few things are more durable than solid gold. Unlike their flightier cousins, the gases and liquids, solids have regular structures that generally resist deformation. But there are materials that challenge our notions of a solid. They are rigid and strong, yet flexible, incredibly light yet so porous that the surface area of one gram could cover an entire football pitch.

These solids are known as metal–organic frameworks, or MOFs. They have no internal walls, just a bare molecular scaffold, creating a regular, sturdy, crystalline structure that is packed full with empty space. But if the scientists building these structures get their way, the materials will soon be packed full of useful gases, such as compressed hydrogen or methane, making it easier to store and transport these alternative fuels.

Chemists expected that the vast, open

are more easily penetrated than most. Chemists have used porous materials, including clays and zeolites, to trap and store gases for decades. But the pores and channels in naturally occurring porous materials are of

into smaller volumes," says Yaghi. Every advance has made it easier to stuff more gas into the structure, attracting the interest of German chemicals giant BASF, which is about to move its MOF research into small-scale production.

Yaghi is thrilled by BASF's investment in his work. In Yaghi's lab, MOFs can now be

Applications in hydrogen storage, CO_2 sequestration and catalysis

Commercial materials: Basolite (BASF/Sigma-Aldrich)

LIQUID-ASSISTED GRINDING (LAG): SCREENING FOR METAL-ORGANIC ARCHITECTURES

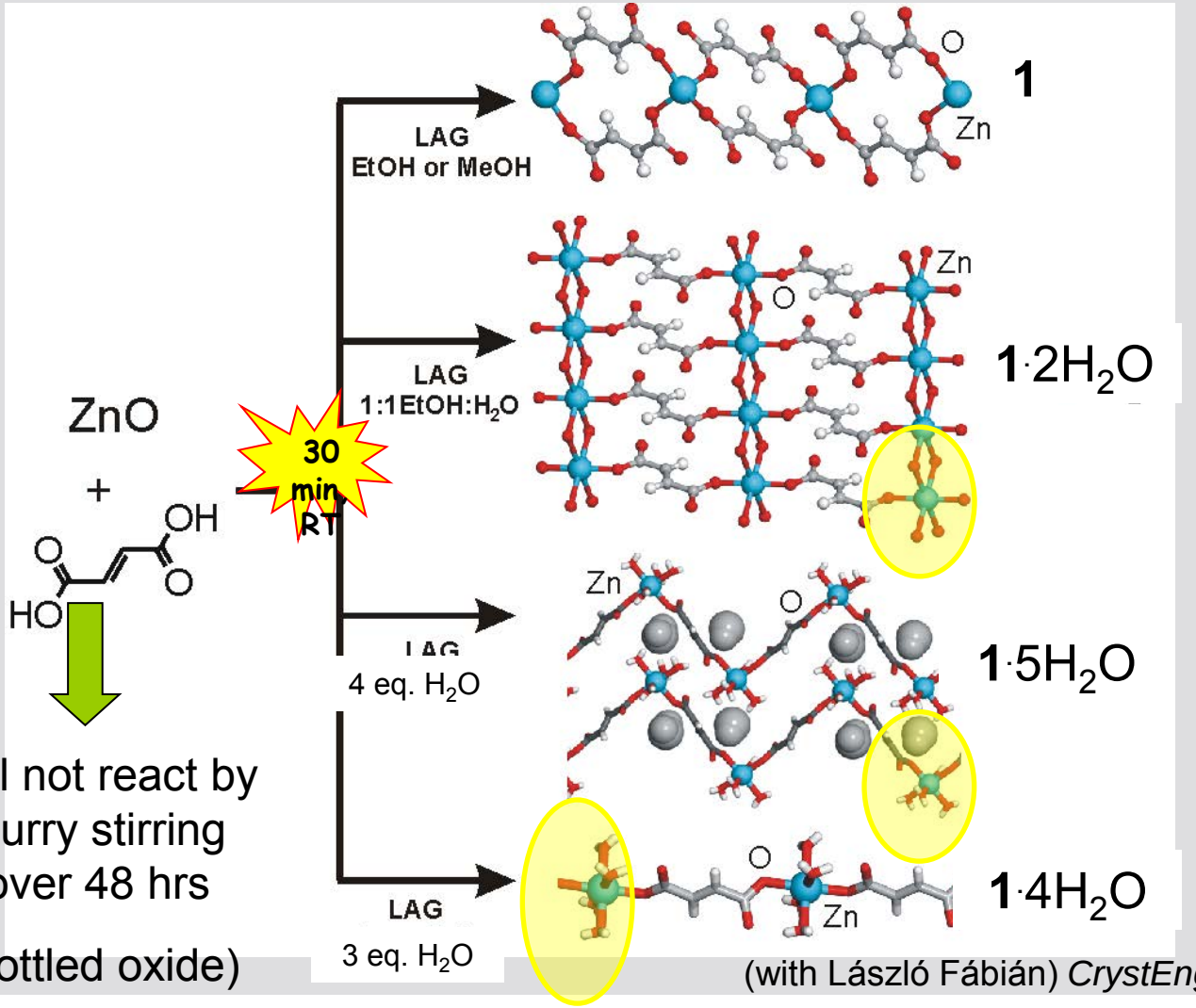

Will not react by slurry stirring over 48 hrs

(bottled oxide)

3-D polymer

previously unknown

2-D polymer (sheets)

previously unknown

1-D polymer (zigzag inclusion host)

forms in solution

1-D polymer (linear chain)

forms in solution

(with László Fábián) *CrystEngComm* **2009**, *11*, 743.

PILLARED MOFS DIRECTLY FROM THE OXIDE

We' d like:

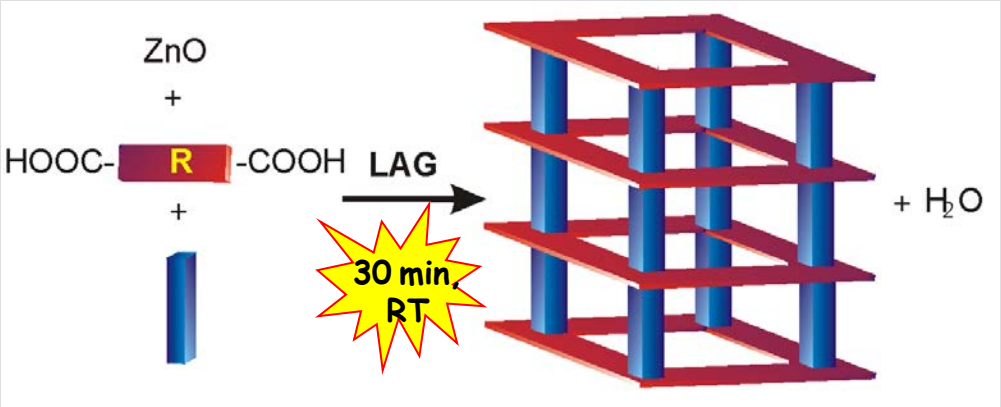

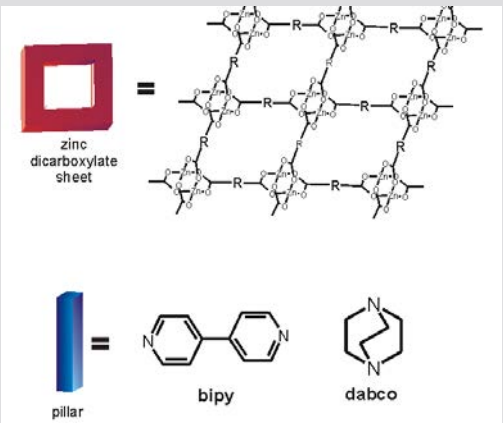

We get:

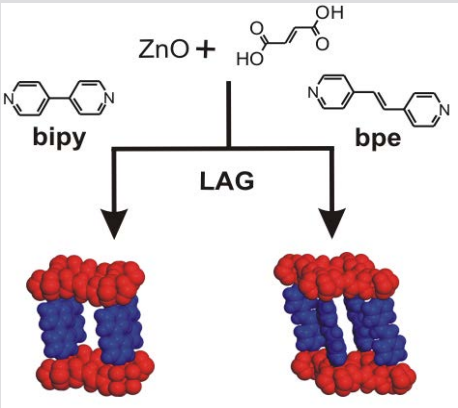

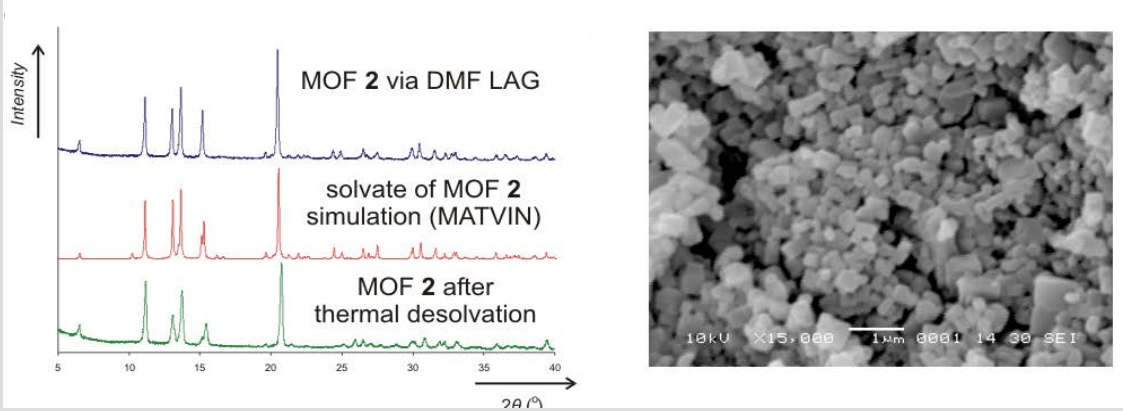

(No rxn by neat grinding)

(with László Fábián *CrystEngComm* **2009**, *11*, 743)

30 min grinding replaces 2 days solvothermal synthesis in DMF, 160 °C

TEMPLATING AND CATALYSIS IN MOF MECHANOSYNTHESIS

ILAG: ion- and liquid- assisted grinding

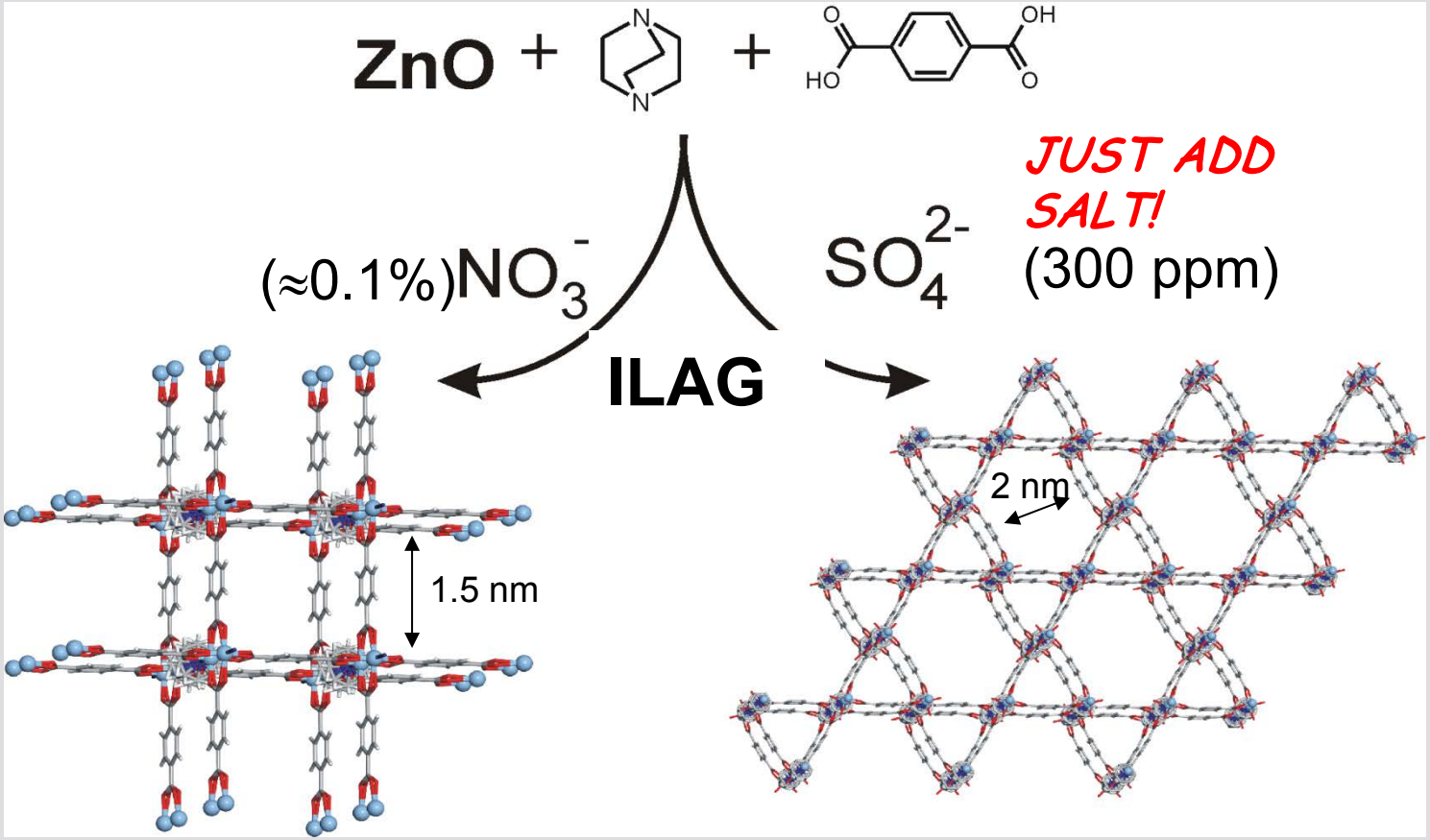

Angew. Chem. Int. Ed. **2010**, 49, 712.

ZEOLITIC IMIDAZOLATE FRAMEWORKS (ZIFS)

The bent geometry of the imidazole ligand, coupled with the tetrahedral coordination of Zn^{2+} results in a metal-organic analogy of silicate/zeolite structures

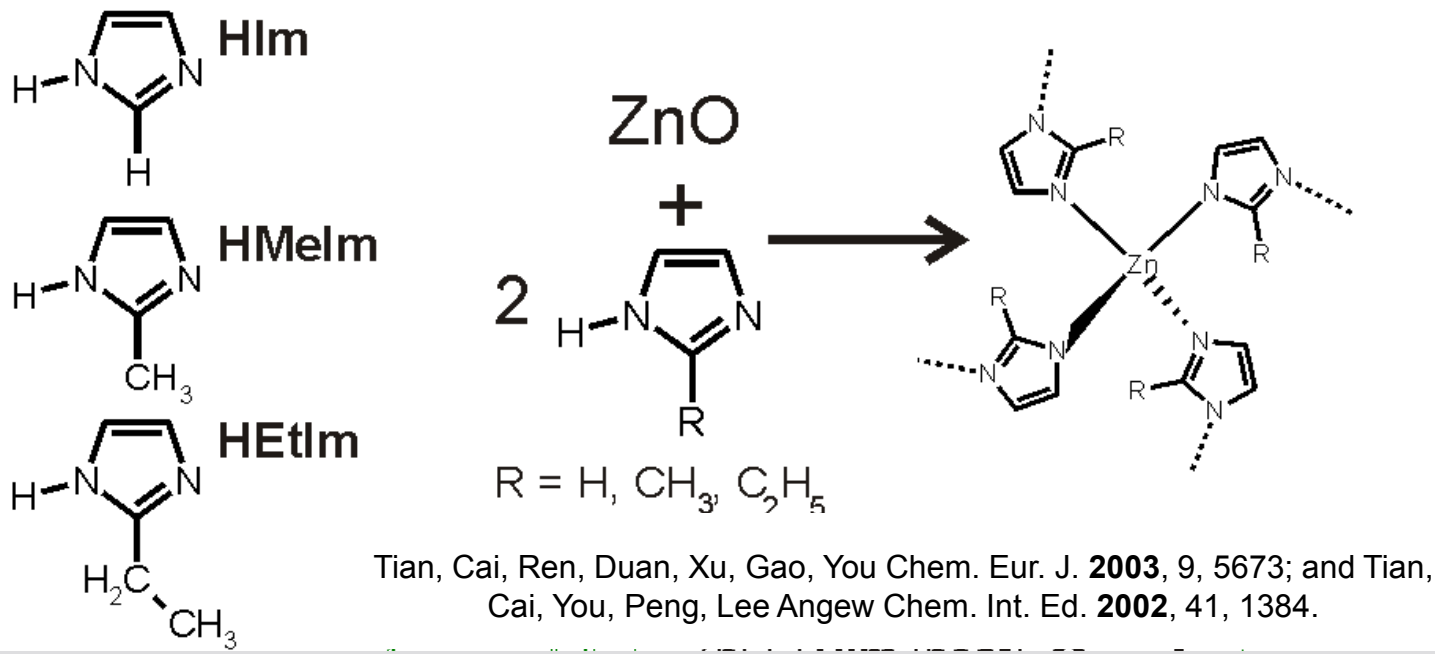

Tian, Cai, Ren, Duan, Xu, Gao, You Chem. Eur. J. **2003**, 9, 5673; and Tian, Cai, You, Peng, Lee Angew Chem. Int. Ed. **2002**, 41, 1384.

Normally obtained through solvothermal synthesis from zinc nitrate and imidazole ligand. Yields often below 40%

Yaghi, Furukawa, Wang *US Pat. Appl. No.* US **2010**/0186588 A1 (07/29/2010)

Park, Ni, Coté, Choi, Huang, Uribe-Romo, Chae, O'Keeffe, Yaghi *Proc. Natl. Acad. Sci.* **2006**, *103*, 10186.

EFFICIENCY AND TEMPLATING OF ZIF SYNTHESIS USING LAG/ILAG

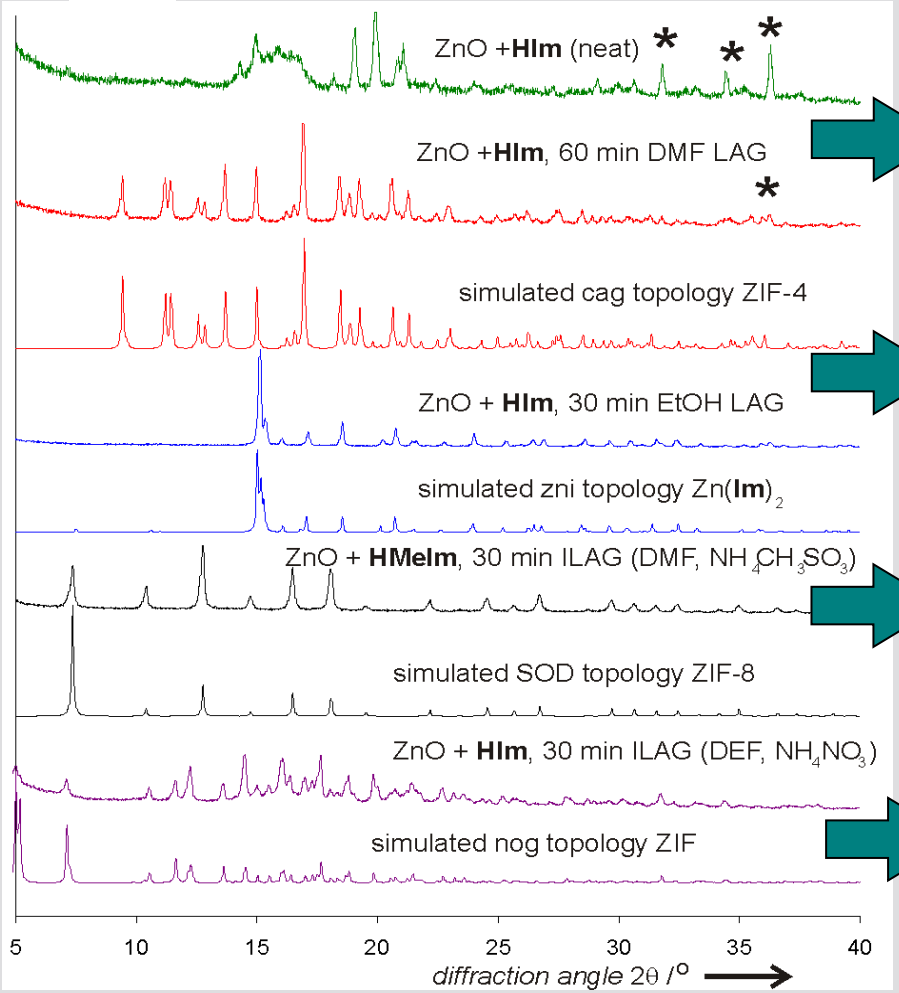

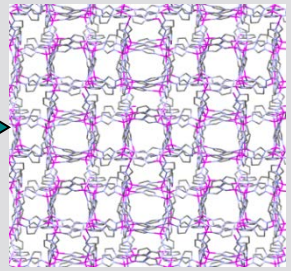

(non-porous)
zni topology

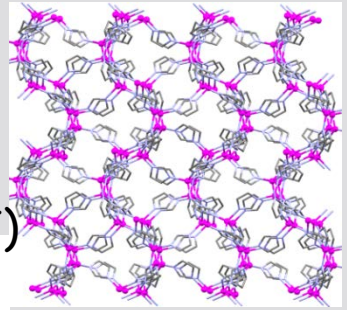

cag topology
(templated by DMF)

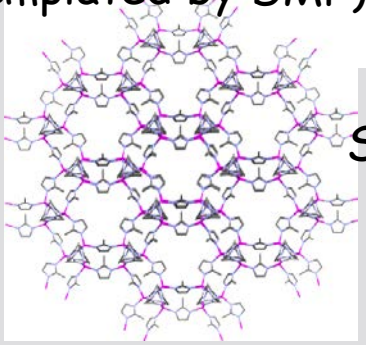

SOD topology

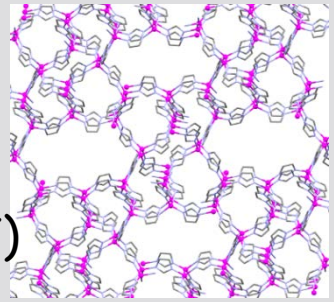

nog topology
(templated by DEF)

Angew. Chem. Int. Ed. **2010**, 49, 9640.

DISCOVERY OF NEW MATERIALS THROUGH ILAG

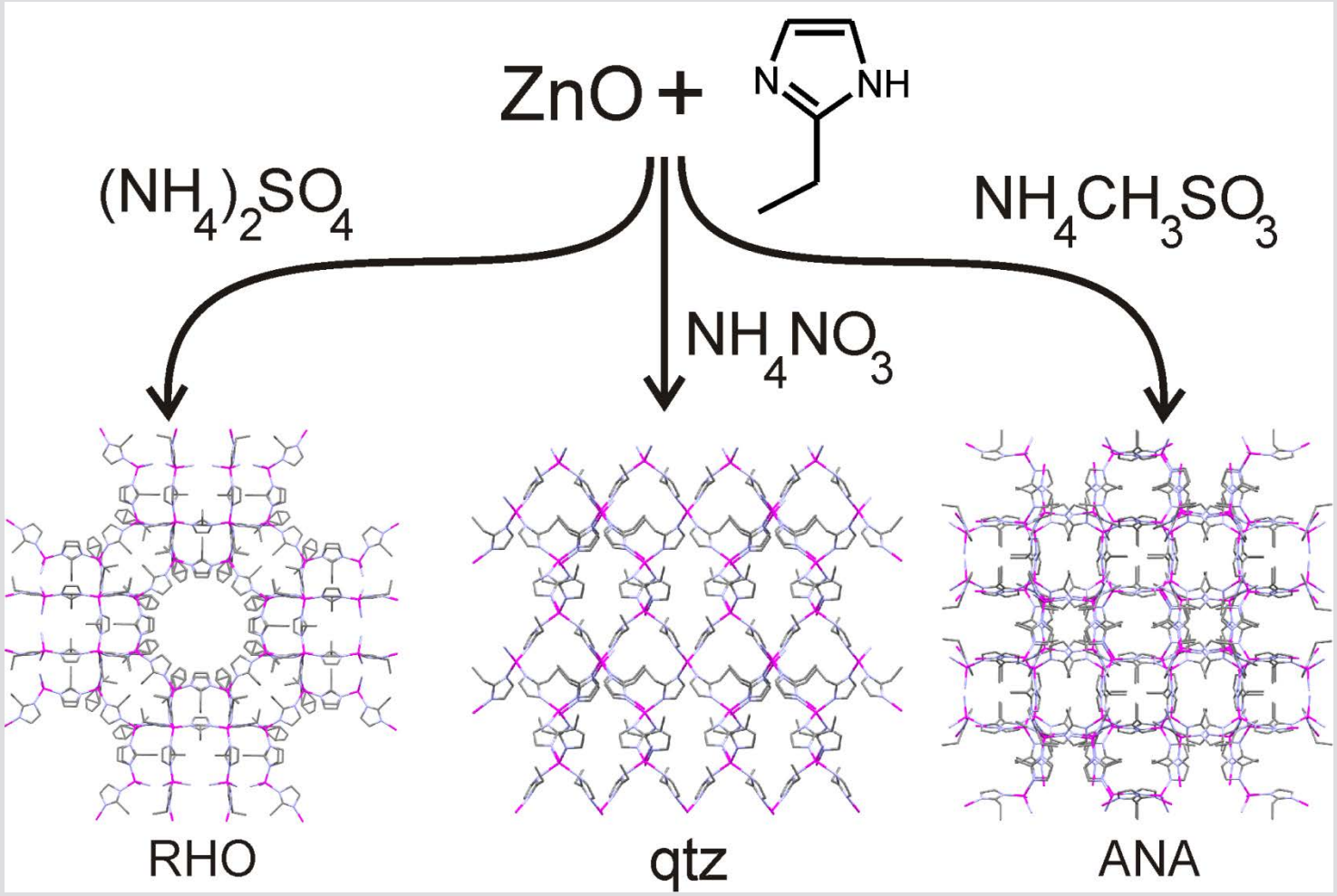

Angew. Chem. Int. Ed. **2010**, 49, 9640.

MECHANISTIC STUDIES – LOOKING INTO THE REACTION

A

B

C

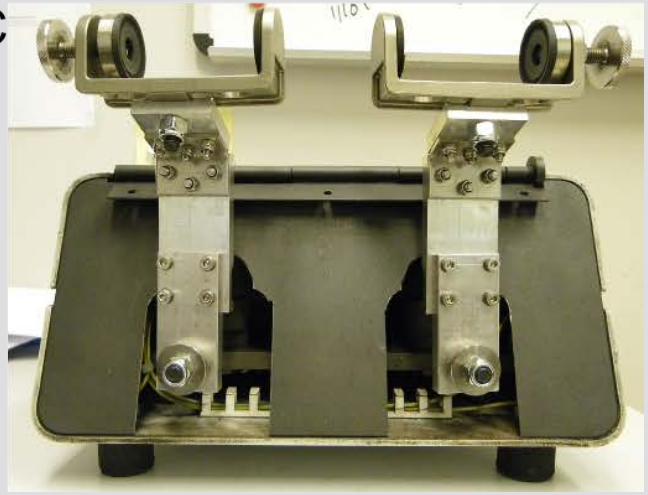

Modified Retsch MM200 mill

MECHANISTIC STUDIES – LOOKING INTO THE REACTION

Visual observation is not very useful - switched to 90 keV X-ray beam at ID15, ESRF, Grenoble

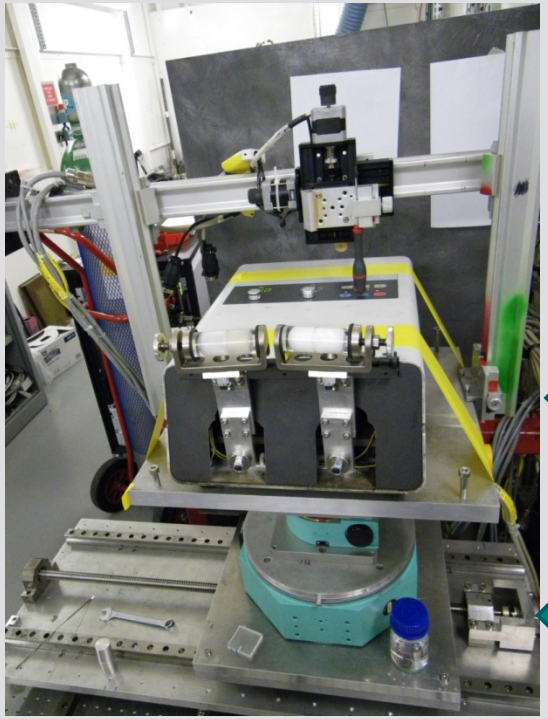

Nature Chem. 2013, 5, 66-73,
also C&EN 2012, 90: "X-ray vision for mechanochemical mills"

MECHANISTIC STUDIES - …

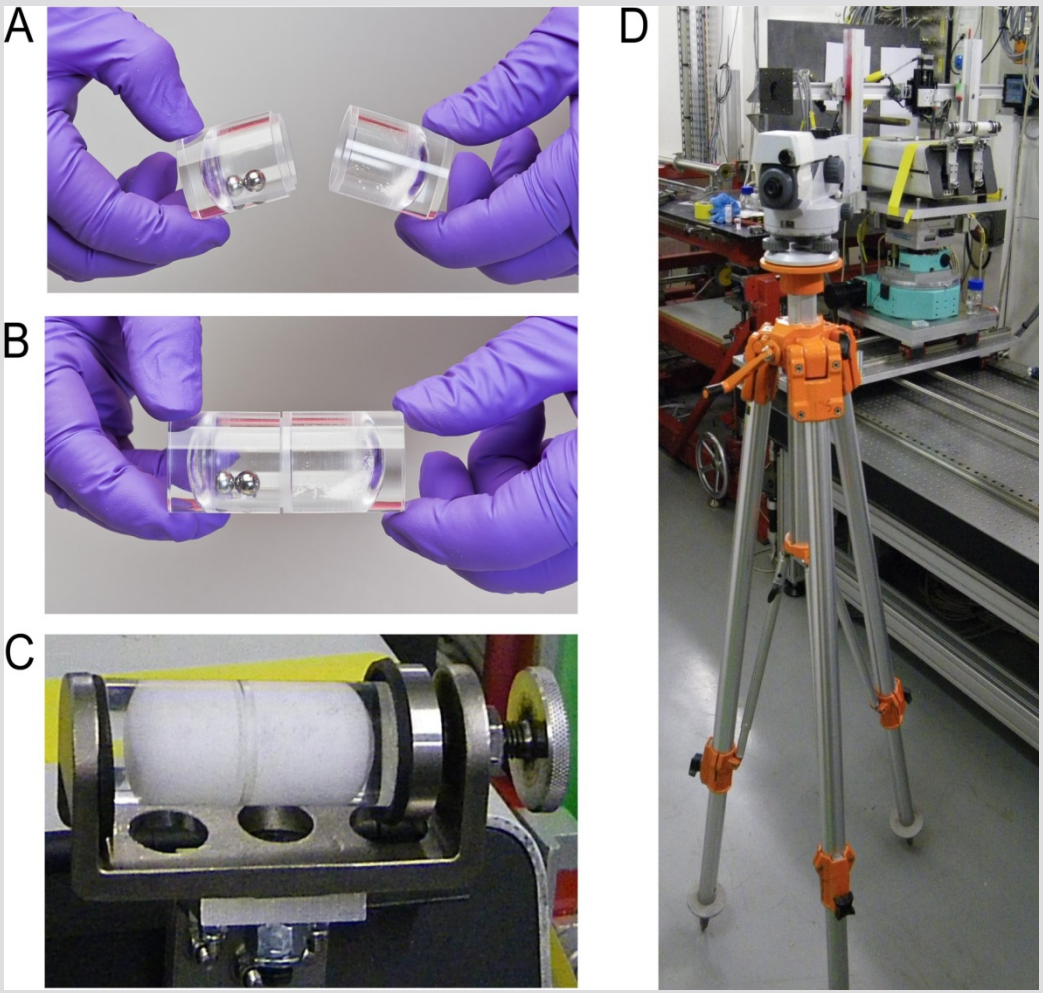

(a) Proper handling of the two halves of the PMMA milling jar before snapping them together.
(b) The milling jar after snapping the two halves together. The left side contains the milling liquid and milling balls. The right side contains the reactants (white powder).
(c) horizontal positioning of the PMMA milling jar on the milling station.
(d) the positioning of the mill and the milling jar with respect to the X-ray beam is verified using a teodolite.

FORMATION AND TRANSFORMATION OF FRAMEWORK TOPOLOGIES

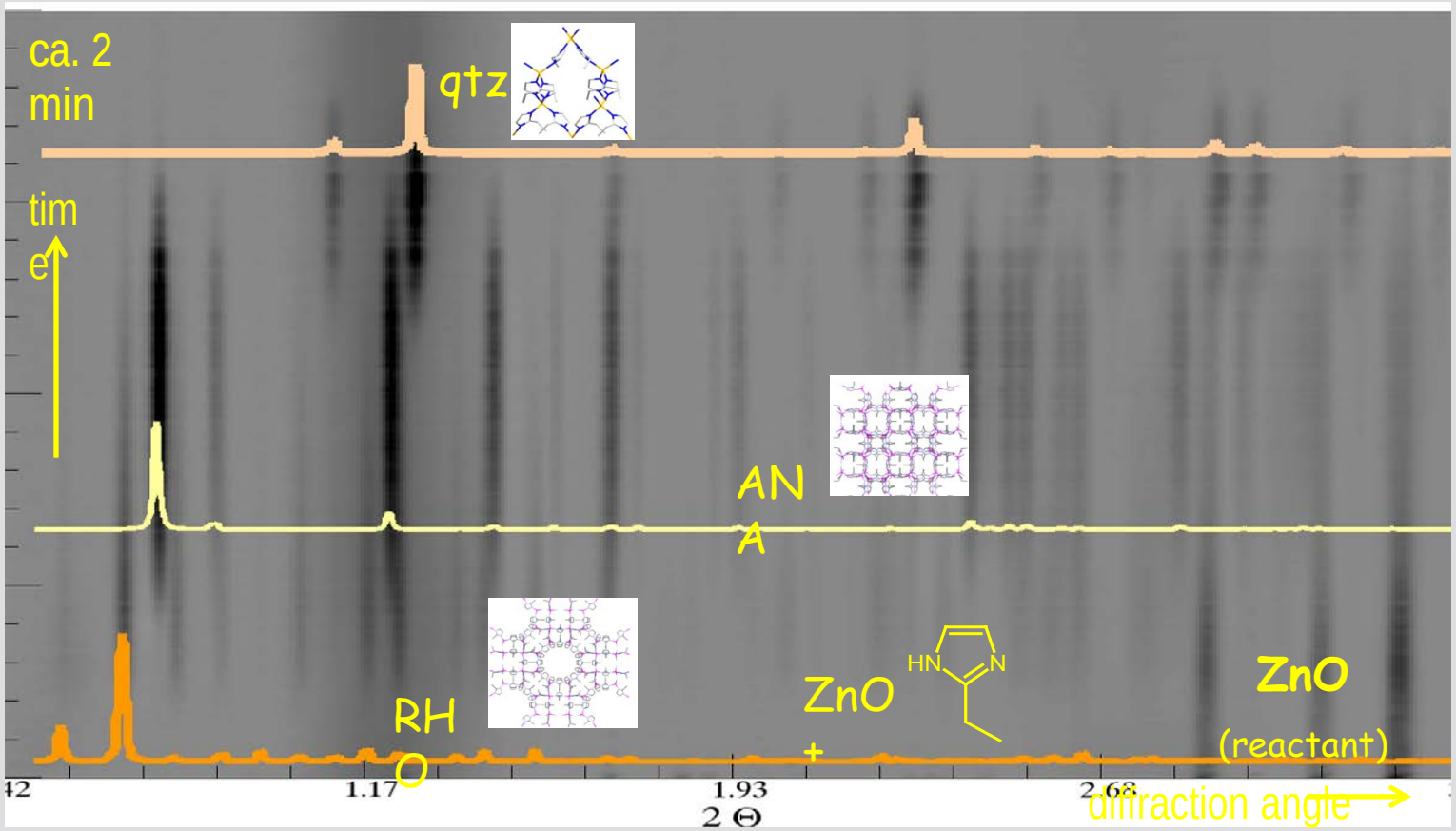

In situ measurements will provide mechanistic detail on the formation, transformation and stabilization of different framework types

THE NEED FOR PROPER SCALING…

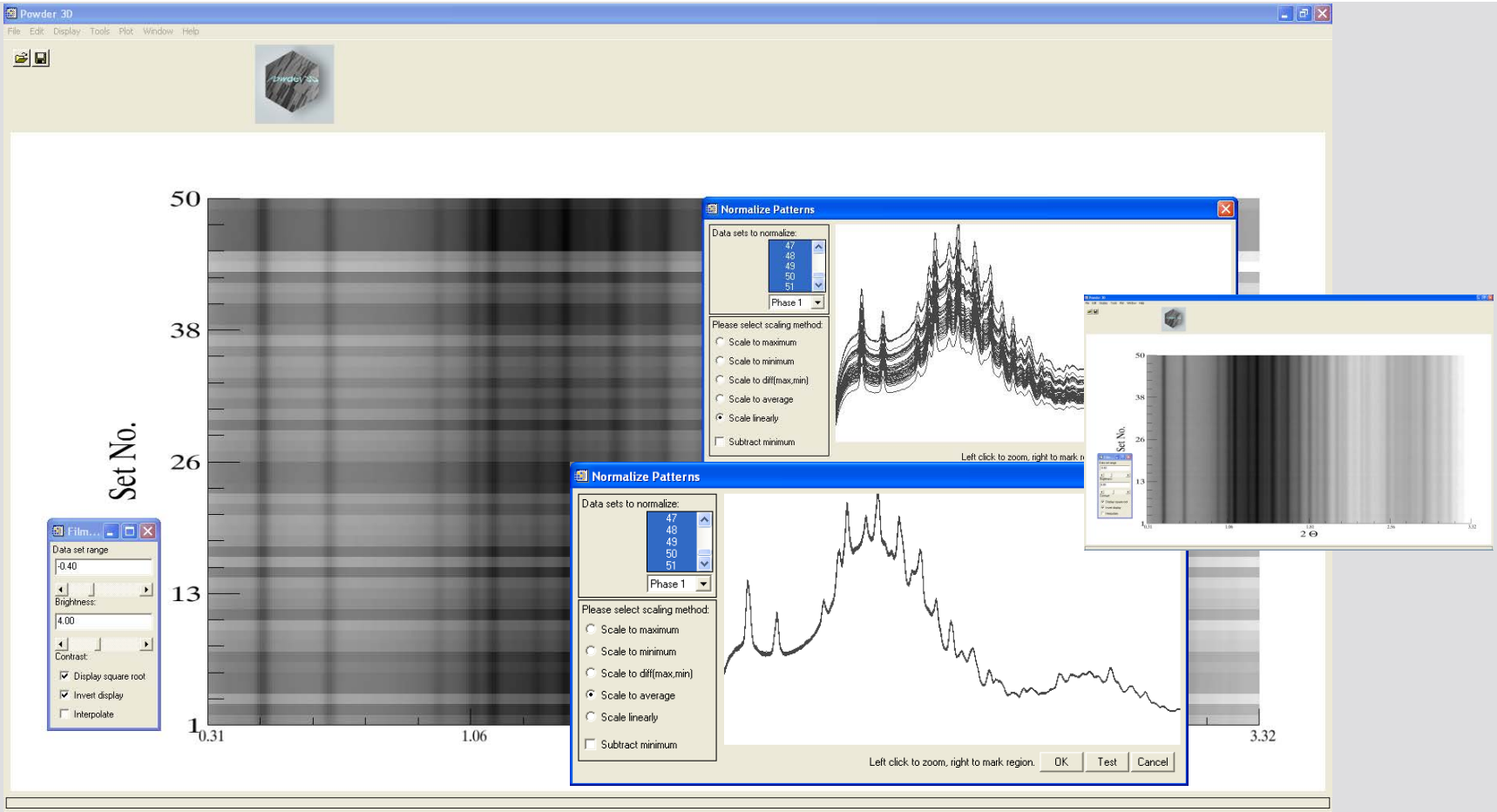

B. Hinrichsen, R.E. Dinnebier, M. Jansen, Powder3D, An easy to use program for data reduction and graphical presentation of large numbers of powder diffraction patterns, 2006, Z. Krist.,Supplement Issue 23 (EPDIC-9 proceedings), 231-236.

INTERMEDIATES AND KINETIC ANALYSIS USING TIME-RESOLVED PXRD

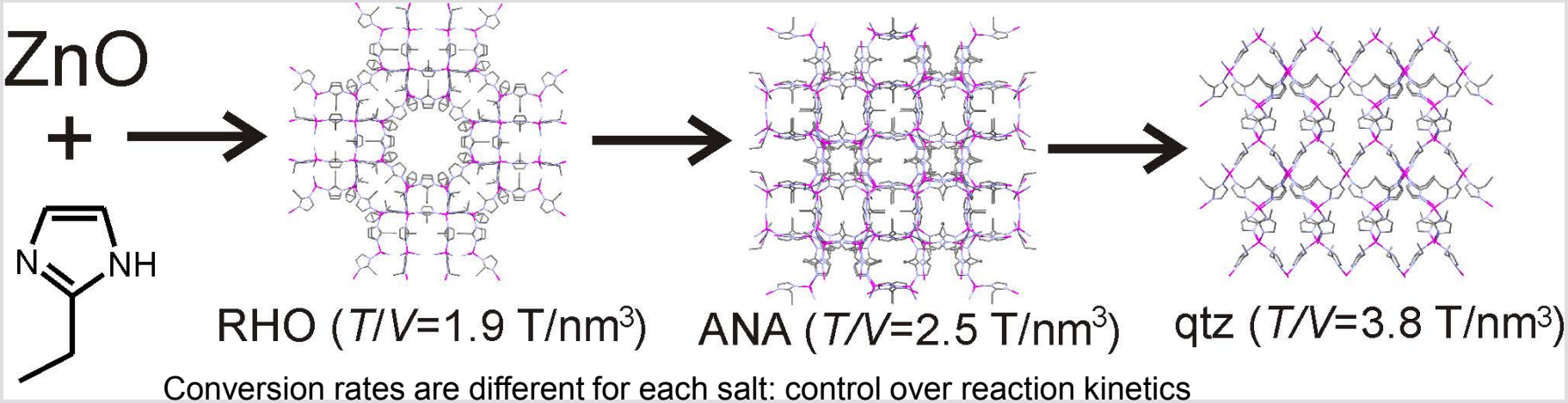

More liquid

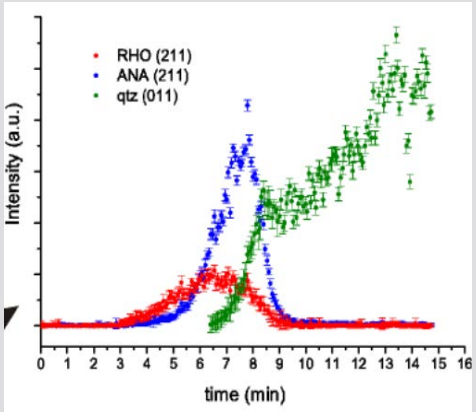

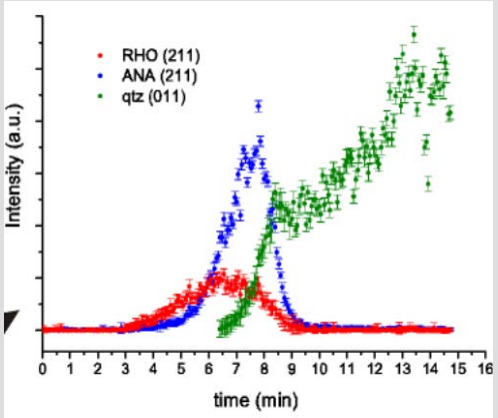

Less liquid

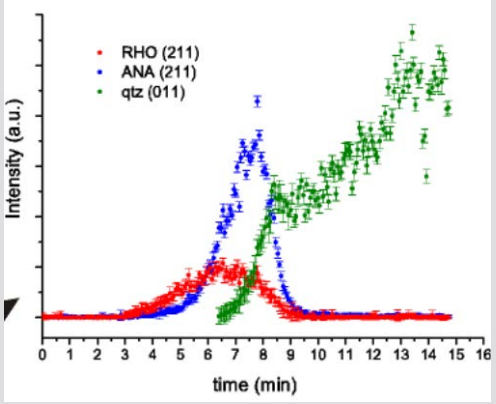

Direct monitoring of how reaction kinetics is affected by different parameters

PARTICLE SIZE EVOLUTION BY TIME-RESOLVED PXRD

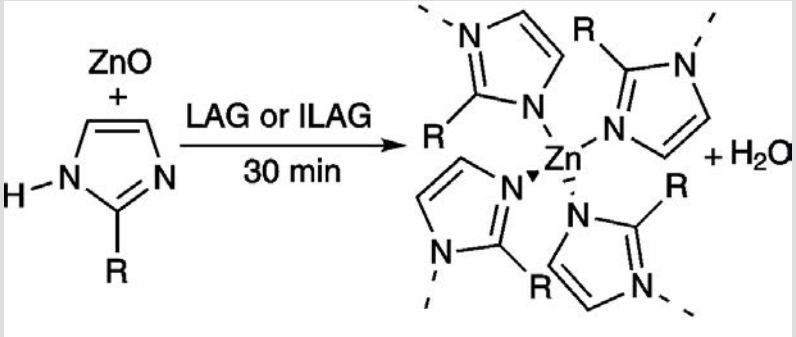

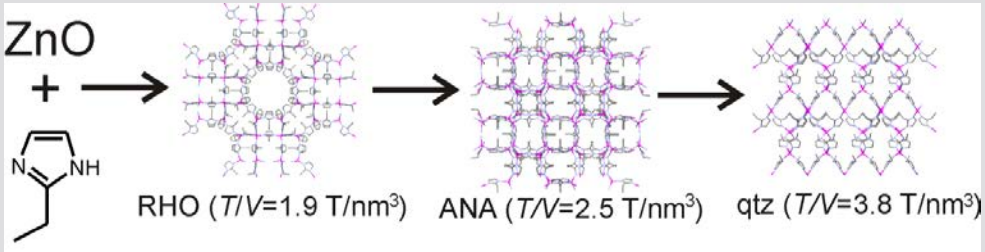

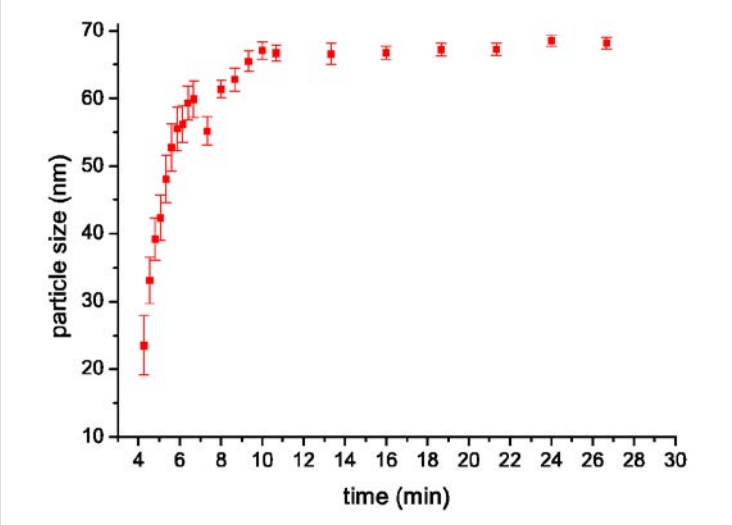

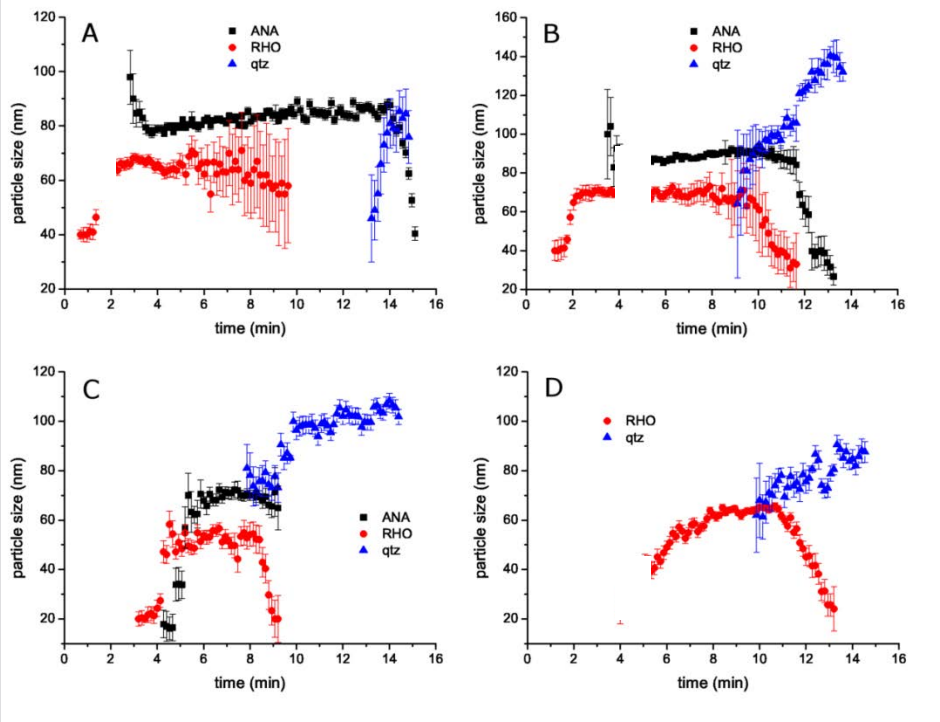

Direct monitoring of how particle size changes throughout milling

NOVEL CHARACTERIZATION OF THE ADSORPTION SITES IN LARGE PORE METAL-ORGANIC FRAMEWORKS: COMBINATION OF X-RAY POWDER DIFFRACTION AND THERMAL DESORPTION SPECTROSCOPY

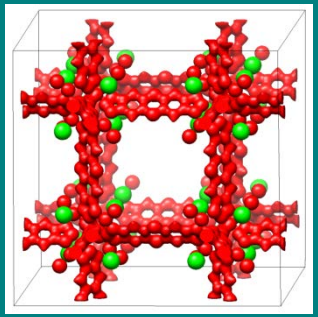

Soleimani-Dorcheh, A., R. E. Dinnebier, A. Kuc, O. Magdysyuk, F. Adams, D. Denysenko, T. Heine, D. Volkmer, W. Donner and M. Hirscher

2012, Physical Chemistry Chemical Physics 14, 37, 12892-12897

SELECTED MOF'S

HKUST-1

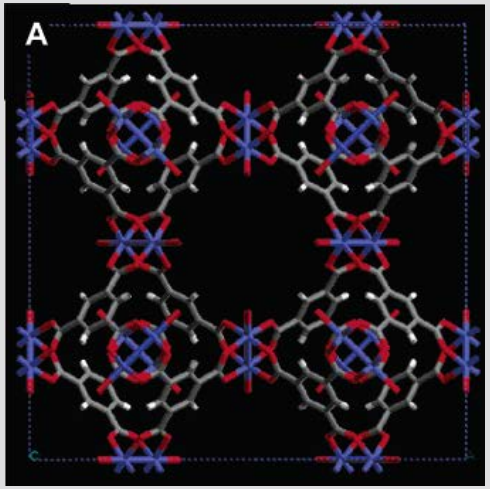

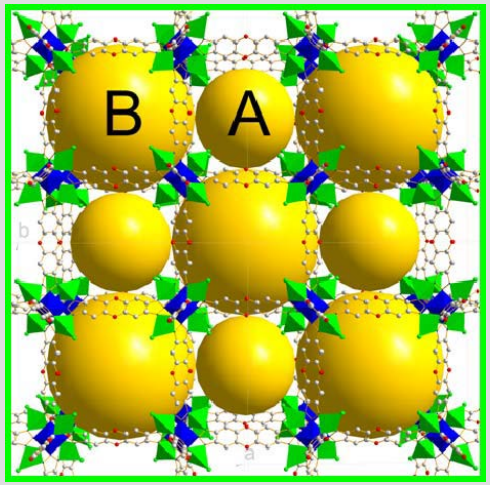

MFU-4l

COF-102

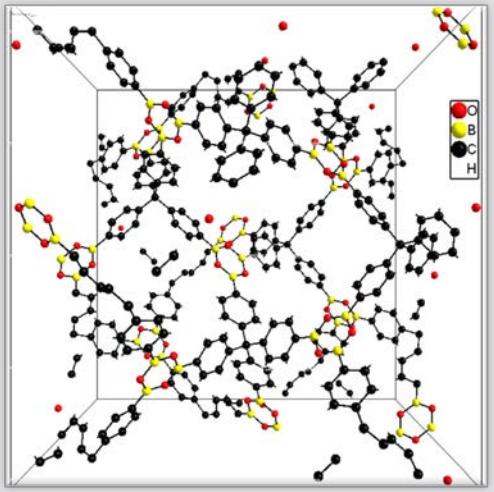

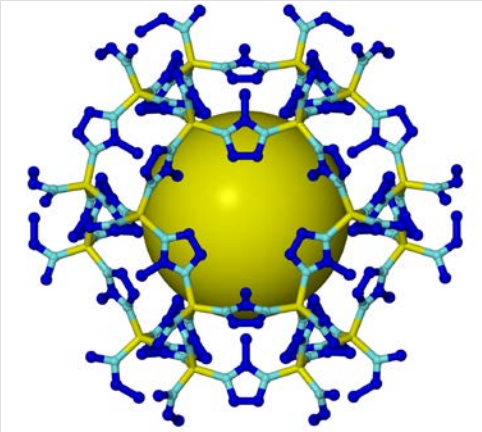

ZIF-8

KR AND XE DESORPTION SPECTRA

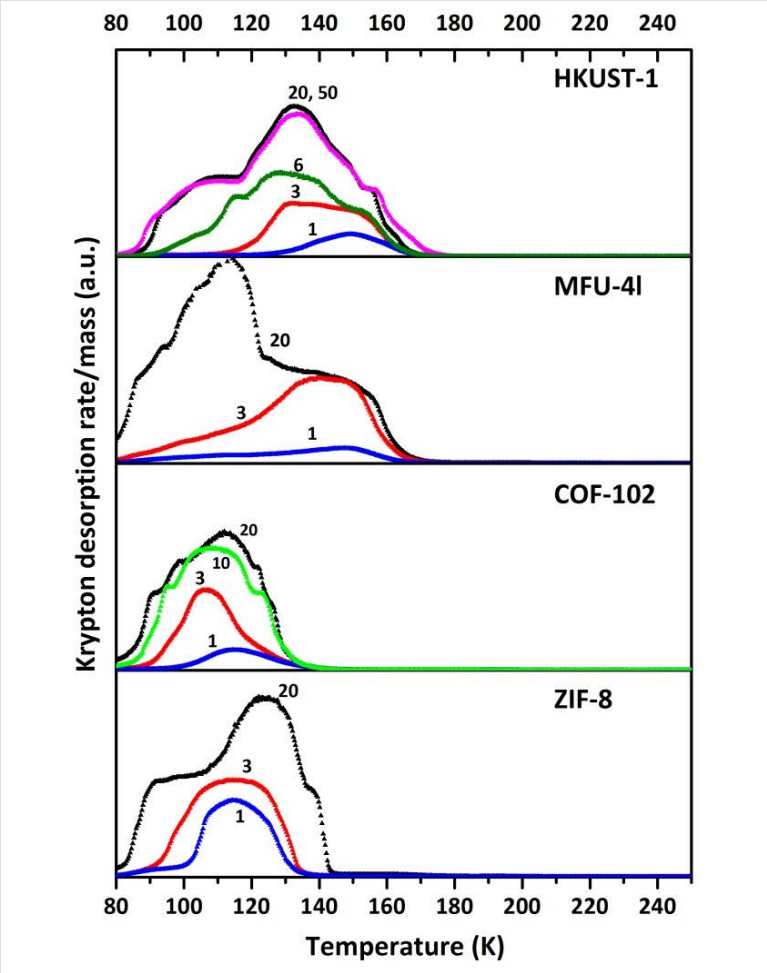

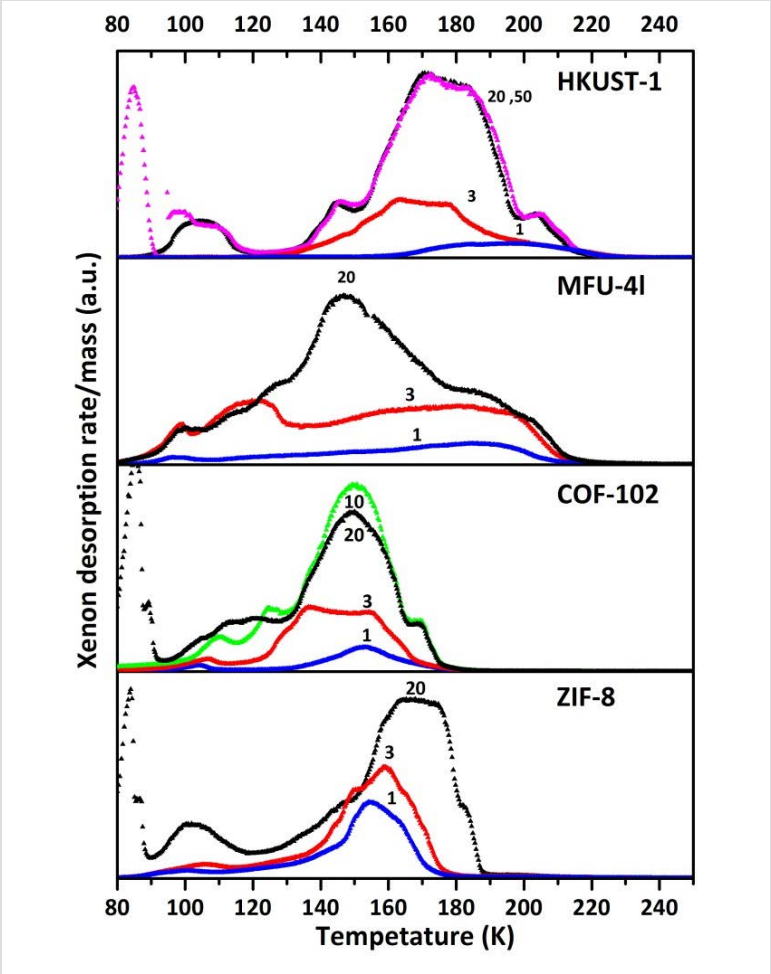

UPTAKE AND DESORPTION TEMPERATURE

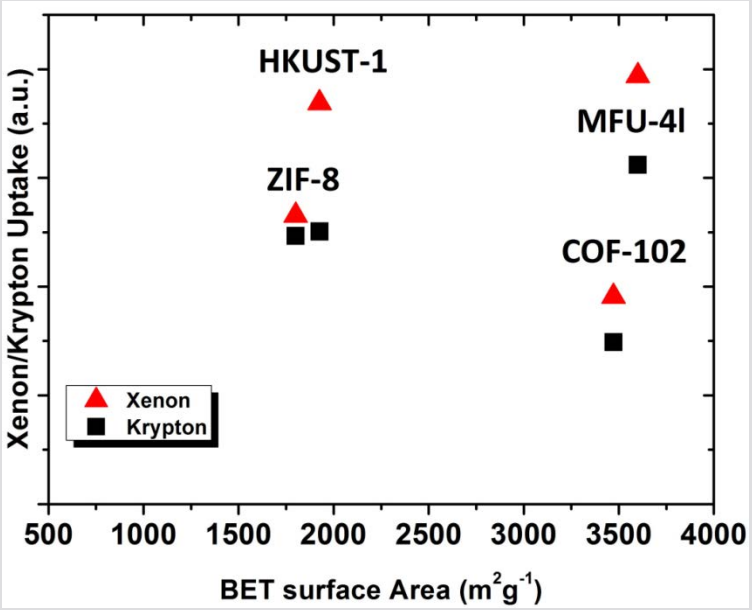

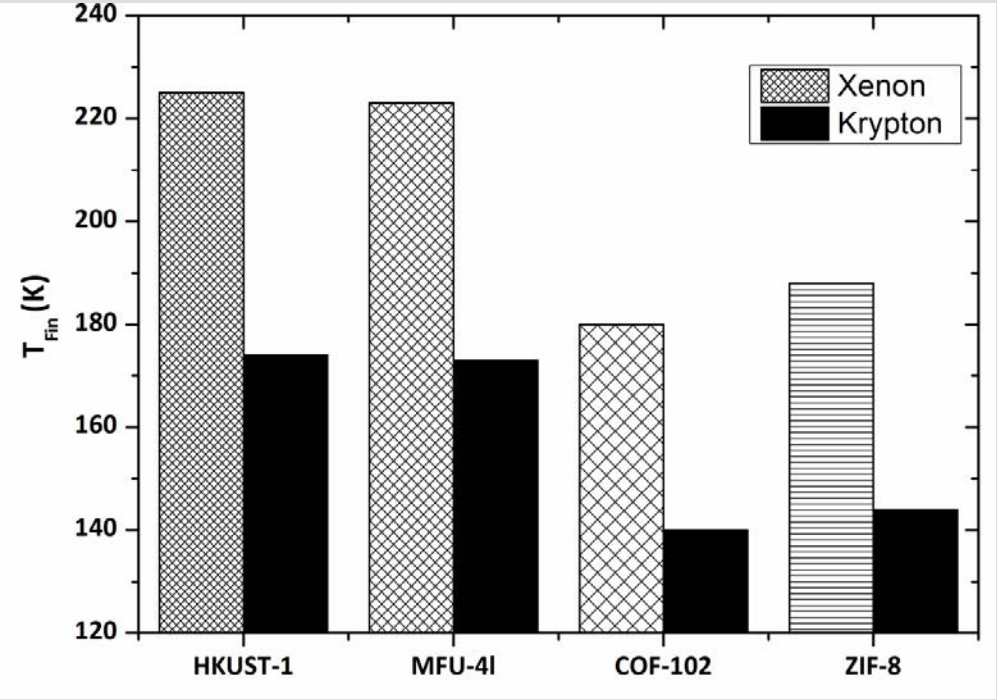

Microporous and Mesoporous Materials, **162** (2012) 64

ADSORPTIONS ISOTHERMEN

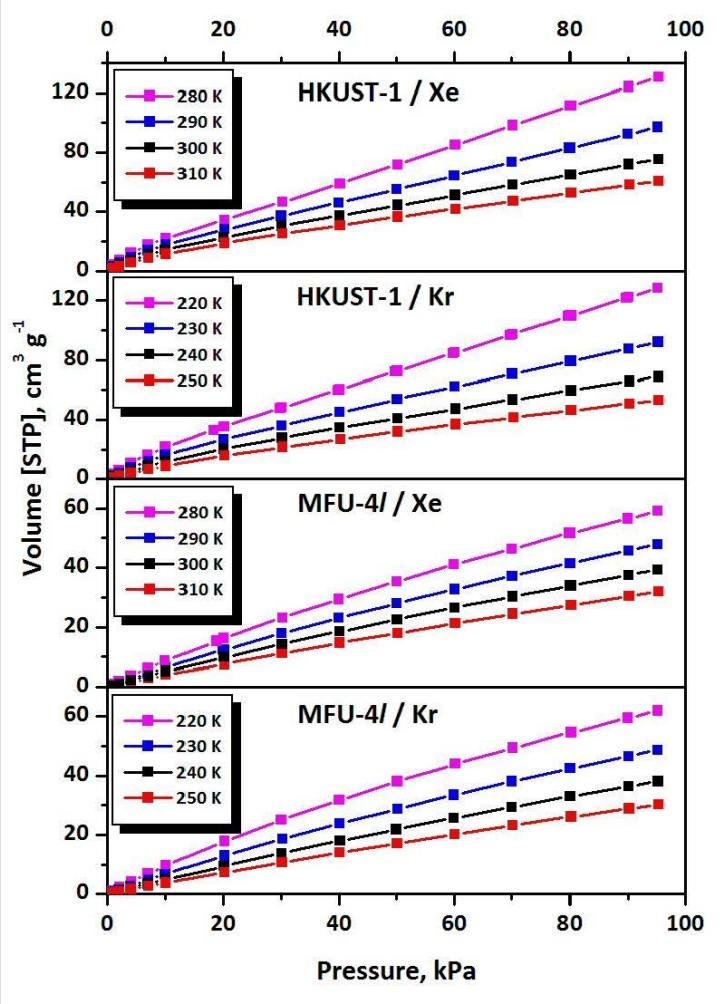

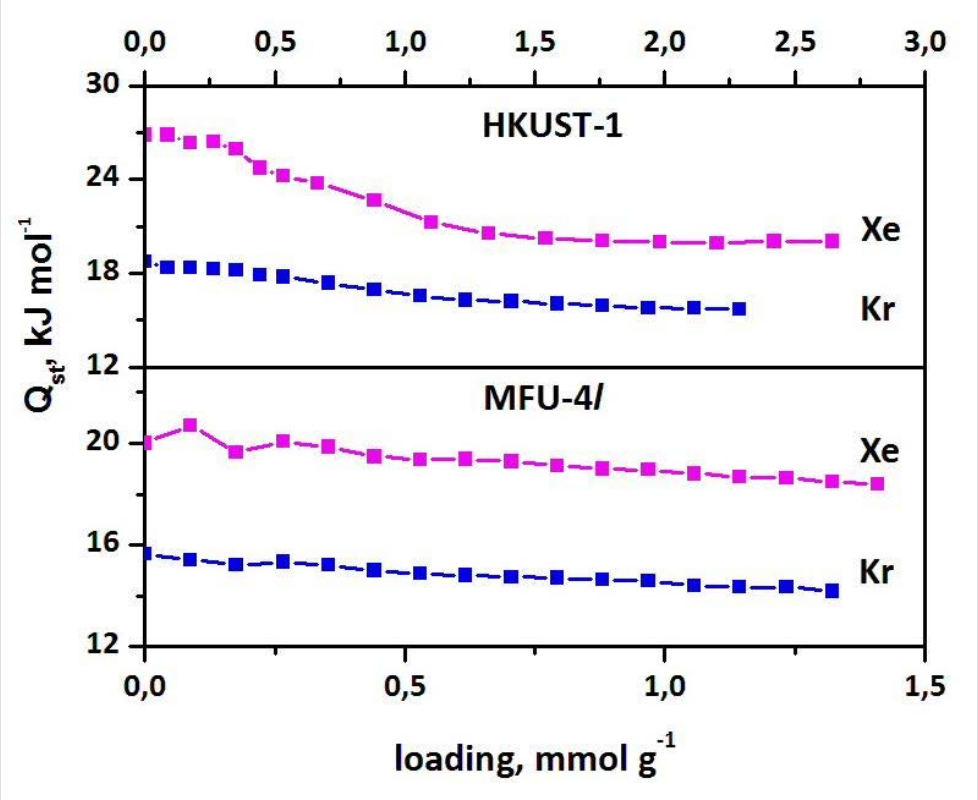

XENON ADSORPTION SITES IN MFU-4L

Methods:

1. Thermal desorption spectroscopy
2. In-situ X-ray powder diffraction
3. Quantum mechanical calculation

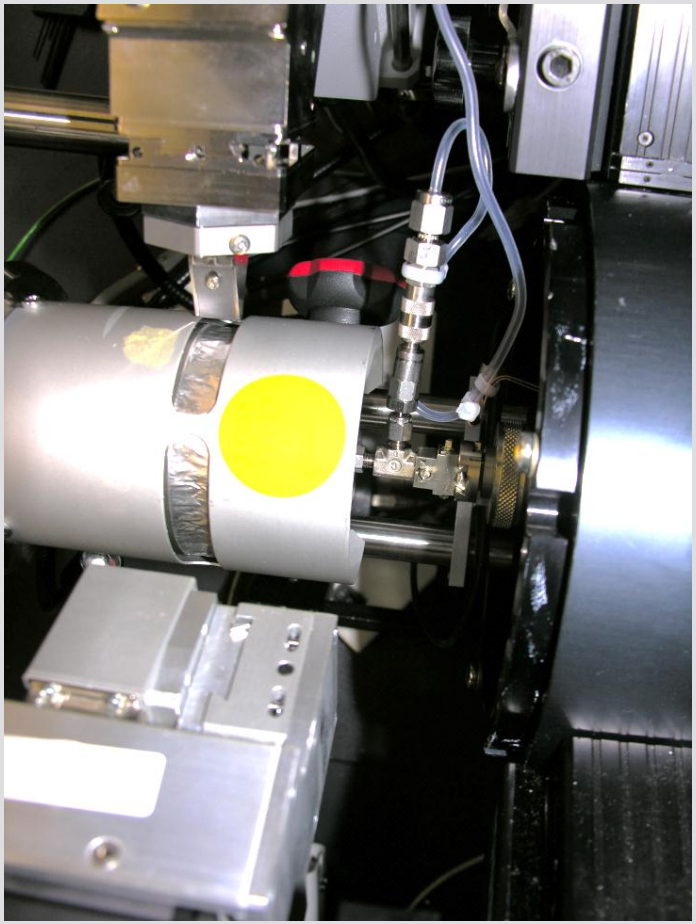

XE ADSORPTION ON MFU-4*LARGE*

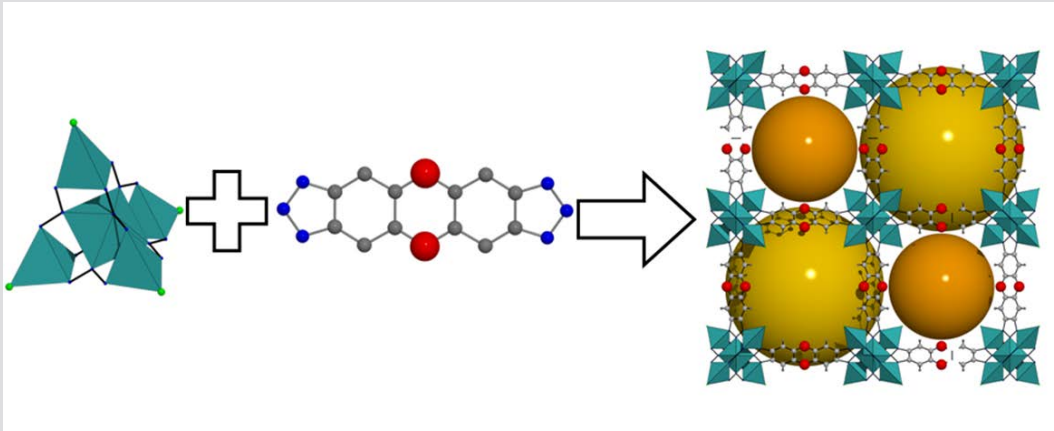

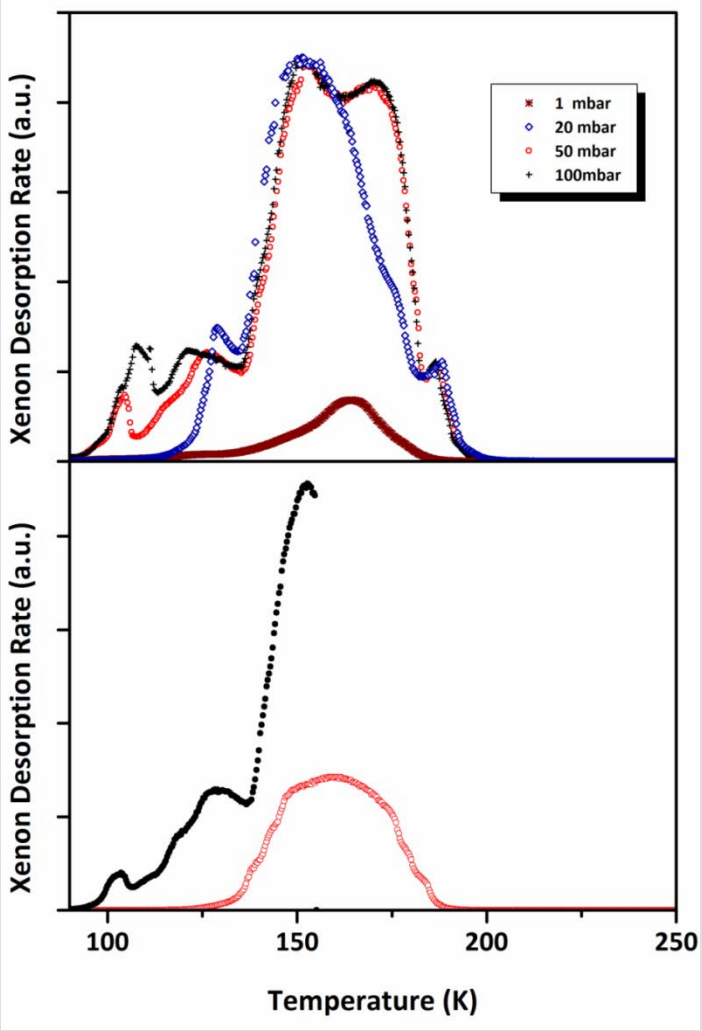

In-situ X-ray Powder Diffraction on MFU-4l

- Loaded at 20mbar
- Different patterns at 110 and 150K
- **Only one** adsorption site for Xenon at 2/3,2/3,2/3 (32f positions)
- Site Occupancy: at 110K≈100% and at 150K=23%

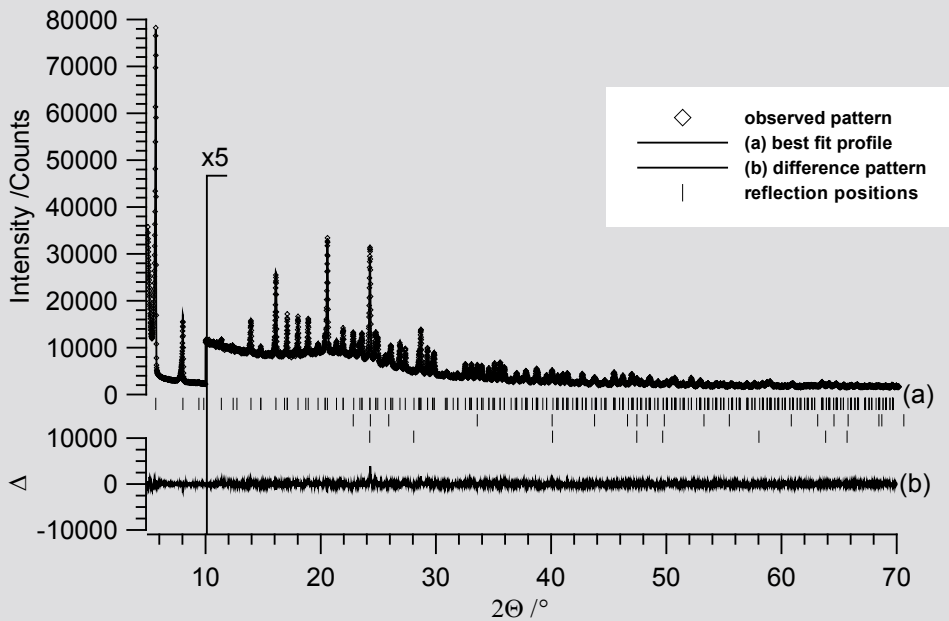

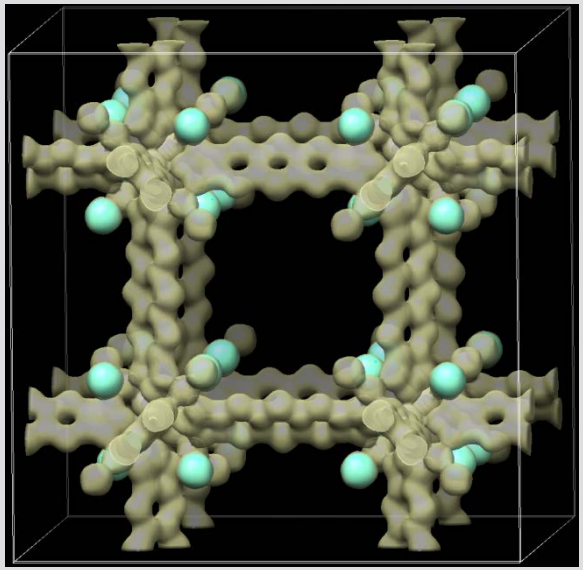

OPTIMIZED DFT CALCULATION

Xenon Adsorption Energy:

Large pore: 96 $KJmole^{-1}$

Small Pore: Equal to Xe-Xe Van der Waals force

Xenon does not adsorb in the small pores!

Unpublished work

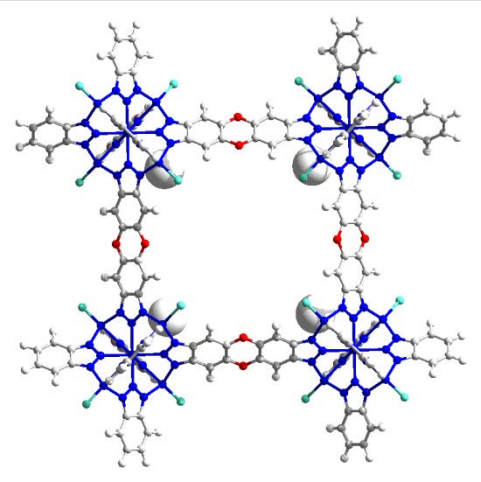

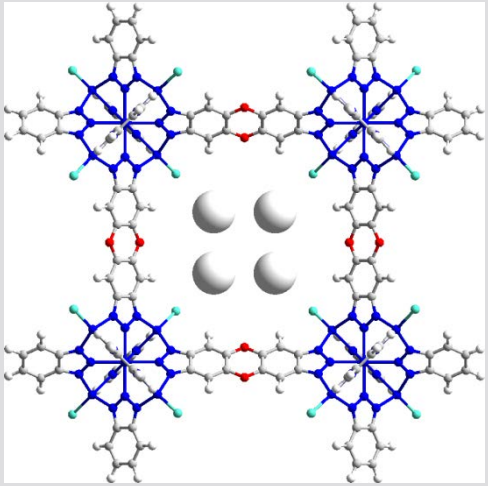

XRD AND THEORY

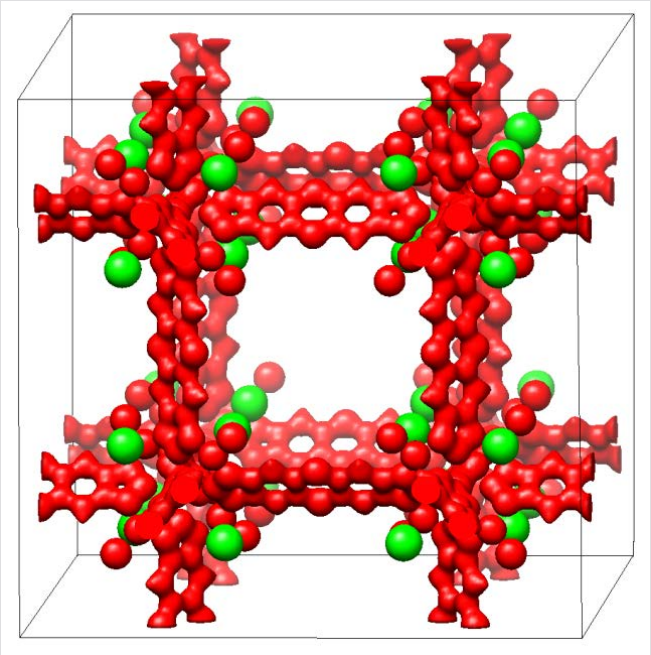

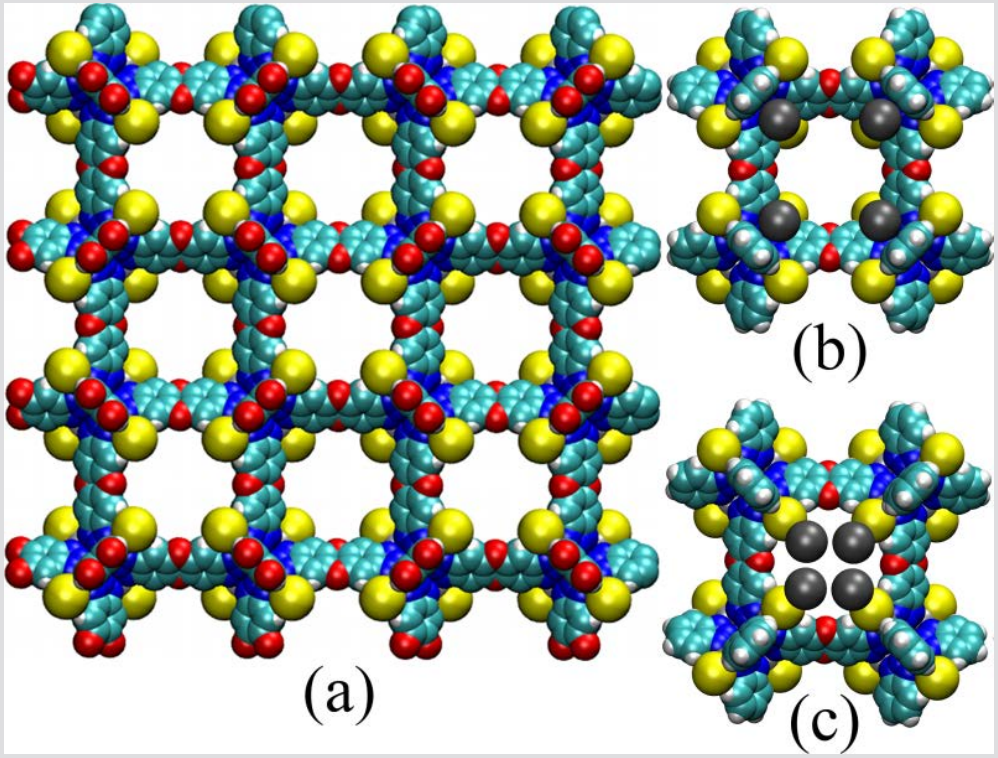

Xe sites from MEM-analysis

Xe sites from DFT calculations

ADVANCES IN THE ANALYSIS OF IN-SITU XRPD DATA USING THE METHOD OF MAXIMUM ENTROPY (MEM)

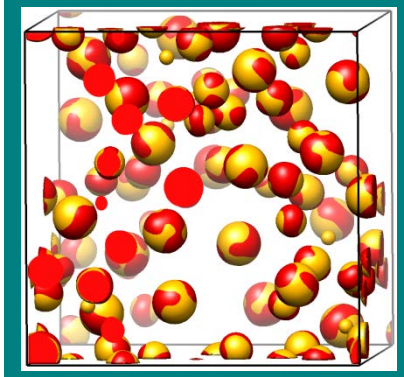

Oksana Magdysyuk, Ali Samy, Sander van Smaalen, Martin Jansen, Pavel Kazin, Robert E. Dinnebier

2010, ACTA CRYST. B, 66, 184-195.

2012, Z. Kristallogr. 227, 321–333.

OUTLINE

- Introduction
- MEM versus Fourier analysis
- The effect of biasing
- Selected Examples
- Using the MEM to
  - locate intercalated atoms with low occupancy
  - analyse disorder
- Conclusions

CONCEPT OF MEM

The maximum entropy method (MEM) can be used to extract the maximum amount of information from a limited set of data by maximizing the entropy in an iterative process:

$$S = -\sum_{i=1}^{Npix} \rho_i \ln \frac{\rho_i}{\rho_i^{prior}}$$

$$N_1 \times N_2 \times N_3 = N_{pix}$$

- the electron density is sampled at the points of the grid over the unit cell

$$\rho_i^{prior}$$

- the prior density

Prior density:

1) flat
2) any desirable distribution of the available electrons over the unit cell

THE PROBLEM OF POWDER DIFFRACTION
- SUMMARY -

Powder: Single crystal reciprocal lattice is smeared into spherical shells

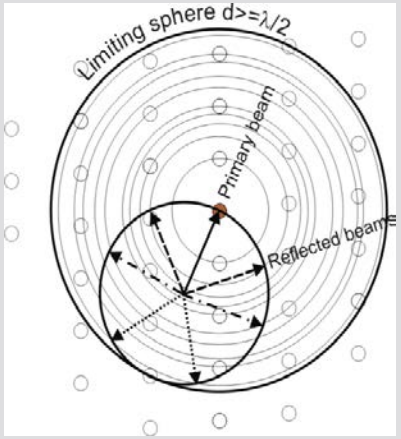

→ $\mathbf{d} \Rightarrow |\mathbf{d}| = d \approx \sin\theta^{-1}$

→Different degrees of overlap:
- multiplicity (just a factor between 2 and 48)
- systematic (e.g. 511, 333 in the cubic case)
- accidental (depending on lattice parameters and scattering angle)

→<u>Not only the phases of the structure factors are unknown, but also many amplitudes</u>

THE PROBLEM OF POWDER DIFFRACTION
- AN EXAMPLE -

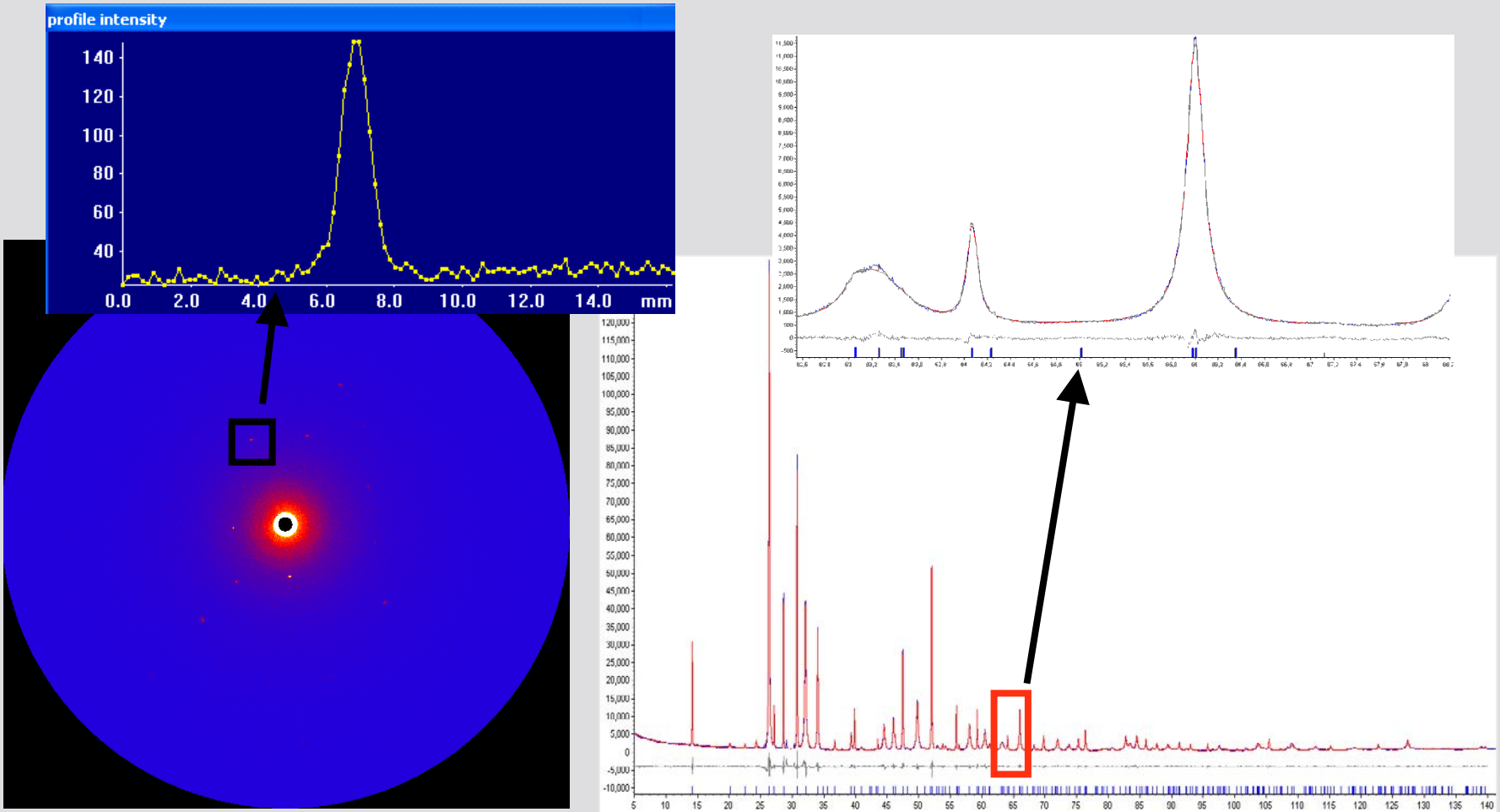

Example: single crystal and powder data of Pb_3O_4

THE GOAL OF THE MEM IS TO FIND THE ELECTRON DENSITY THAT MAXIMIZES THE ENTROPY S SUBJECT TO VARIOUS CONSTRAINTS

1) $$\rho_{total} = \sum_{k=1}^{N_{pix}} \rho_k$$ - normalization of the electron density

2) $$C_F = -1 + \frac{1}{N_F} \sum_{i=1}^{N_F} w_i \left(\frac{\left| F_{obs}(H_i) - F_{MEM}(H_i) \right|}{\sigma(H_i)} \right)^2$$

constraint C_F is based on the observed phased structure factors

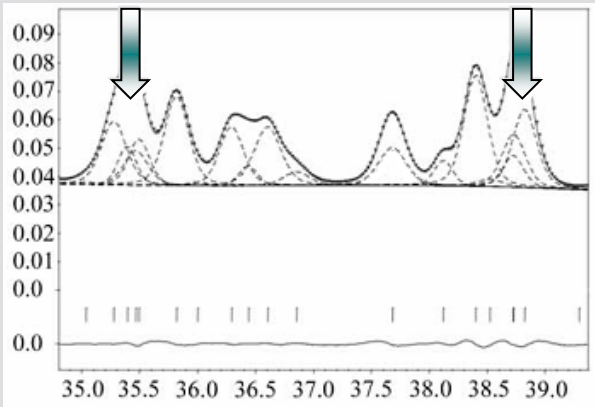

3) $$G^j = \sqrt{\sum_{k=1}^{N_G^j} \frac{m_k \left| F(H_k) \right|^2}{\sum m_k}}$$

constraint G is the "structure factor" of a group of overlapping reflections

$$C_{FG} = -1 + \frac{1}{N_{all}} \sum_{i=1}^{N_F} w_i \left(\frac{\left| F_{obs}(H_i) - F_{MEM}(H_i) \right|}{\sigma(H_i)} \right)^2 + \frac{1}{N_{all}} \sum_{j=N_F+1}^{N_{all}} \left(\frac{\left| G_{obs}^j - G_{MEM}^j \right|}{\sigma(H_i)} \right)^2$$

BASICS OF THE MAXIMUM ENTROPY METHOD (MEM)

Maximize:

$$Q(\rho) = S(\rho) - \sum_{j=1}^{N_c} \lambda_j C_j(\rho), \quad \longrightarrow \quad \frac{\partial Q}{\partial \rho_i} = 0$$

$$\rho_i = \frac{N_{el} N_{pix}}{V} \tau_i \exp\left(-\lambda_F \frac{\partial C_F}{\partial \rho_i}\right) \Big/ \sum_{i=1}^{N_{pix}} \tau_i \exp\left(-\lambda_F \frac{\partial C_F}{\partial \rho_i}\right) \qquad (3)$$

Set of N_{pix} *nonlinear equations*

$$\tau_i^{n+1} \approx \rho_i^{n}$$

Approximation for next iteration

ρ_i	Electron density
τ_i	Prior density
N_{pix}	no of pixels of cell volume V
N_{el}	no of electron/unit cell = F000
w	weight factor
$\sigma(H)$	standered error of F_{obs}
F_{obs}	observed structure factors
F_{MEM}	MEM structure factors
λ	Lagrange multipliers
Nc	no of constraints

Iteration:

$$\rho_i^{n+1} = \frac{N_{el} N_{pix}}{V} \rho_i^{(n)} \exp\left(-\lambda_F \frac{\partial C_F}{\partial \rho_i}\Big|_{\rho_i^{(n)}}\right) \Big/ \sum_i \rho_i^{(n)} \exp\left(-\lambda_F \frac{\partial C_F}{\partial \rho_i}\Big|_{\rho_i^{(n)}}\right)$$

Sakata & Sato algorithm (1990)

The iteration is started with $\rho_i^{(1)} = \tau_i$ and the new density $\rho_i^{(n+1)}$ is calculated from the prior density $\rho_i^{(n)}$, the value of the constraint decreases each cycle untile the condition of $C_F \leq 1$ is fulfilled

POWDER DIFFRACTION: OVERLAPPING REFLECTIONS

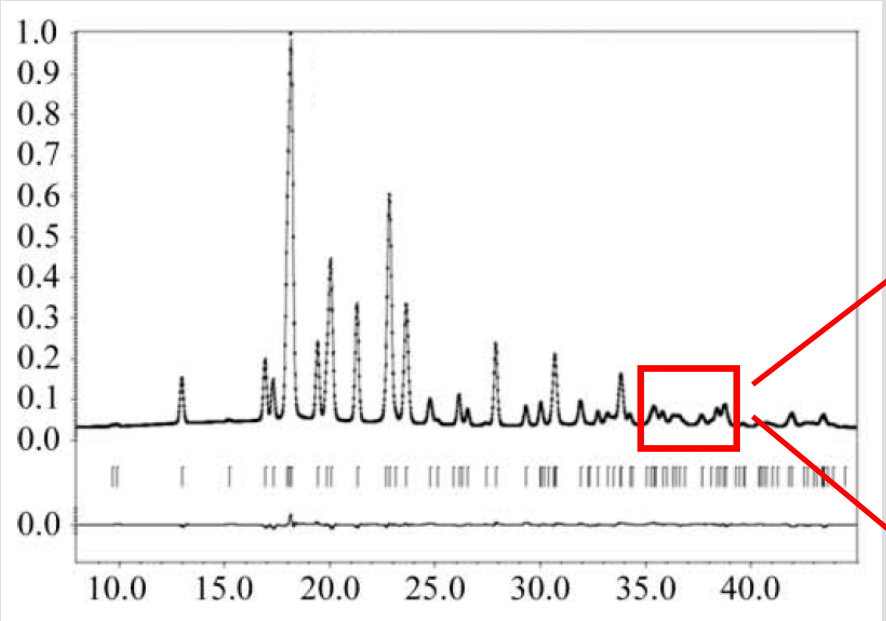

$K_2C_2O_4$

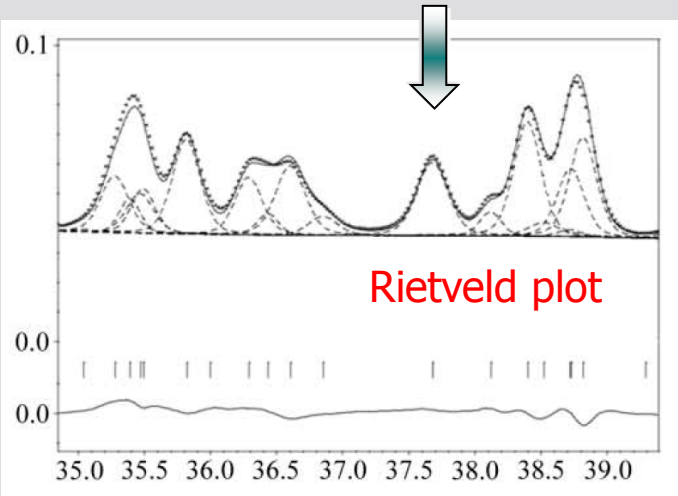

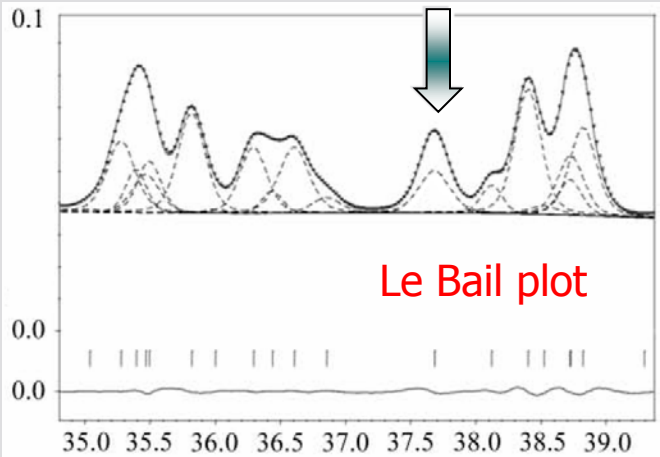

PROFILE ANALYSIS OF X-RAY POWDER PATTERN

<u>Advantages of the Fundamental Parameters Approach (FPA):</u>

In contrast to empirical/conventional profile fitting methods, the refined numerical parameters have physical meaning

FPA greatly reduces the number of parameters refined and hence minimizes parameter correlation

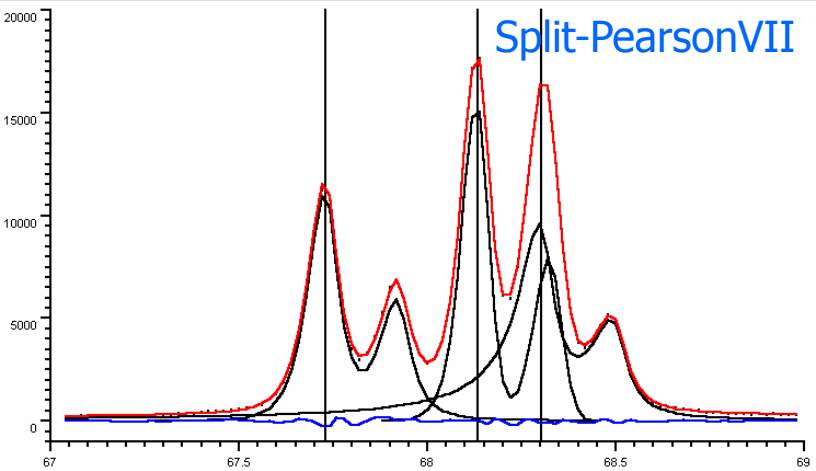

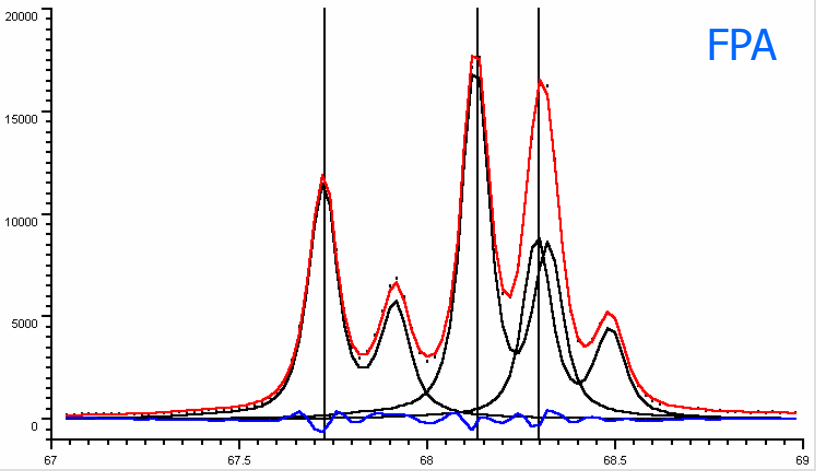

Example: quartz

DECOMPOSITION OF OVERLAPPING REFLECTIONS

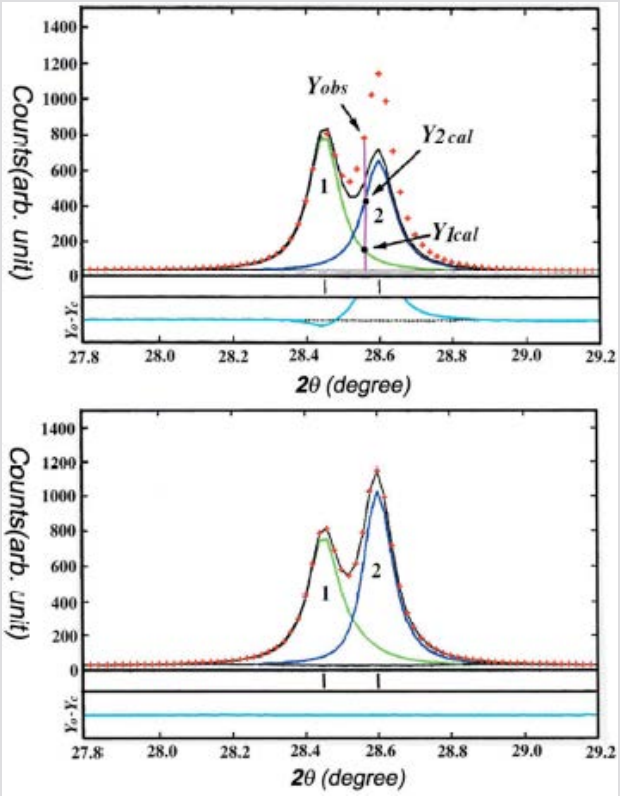

$$Y_i^{obs}(2\theta_j) = \frac{Y^{obs}(2\theta_j)Y_i^{calc}}{\sum_N Y_i^{calc}(2\theta_j)}$$

Rietveld refinement:

- the peak area is proportional to the square of the structure-factor amplitude
- for overlapping peaks, the contribution for a given reflection is weighted by the calculated peak contribution for that reflection divided by the sum of the calculated peak values for each contributing reflection ("F_{obs}" might be wrong)

Le Bail fit:

- there is no initial structural model
- the values of the integrated intensities are determined iteratively after each refinement cycle
- for fully overlapping peaks, intensities are partitioned equally

MEM RECONSTRUCTION OF DIFFERENT TYPES OF ELECTRON DENSITY MAPS FROM POWDER DIFFRACTION DATA

1) F_{calc}, f^{calc} $\xrightarrow{MEM}$ ρ^{MEM}_{calc}

2) F_{obs}, f^{calc} $\xrightarrow{MEM}$ ρ^{MEM}_{obs}

3) $F_{obs}+G$, f^{calc} $\xrightarrow{MEM}$ ρ^{MEM}_{obs+G}

4) $F_{LeBail}+G$, f^{calc} $\xrightarrow{MEM}$ $\rho^{MEM}_{LeBail+G}$

Completely model biased

Least model biased

Dinnebier, R. E.; Schneider, M.; van Smaalen, S.; Olbrich, F.; Behrens U. // ACTA CRYST. 1999. V. B55. P. 35-44.
Samy, A.; Dinnebier, R.E.; van Smaalen, S.; Jansen, M. // ACTA CRYST. 2010. V. B66. P. 184-195.

IER RECONSTRUCTION OF DIFFERENT TYPES OF ELECTRON DENSITY MAPS FROM POWDER DIFFRACTION DATA

1) F_{calc}, f^{calc} $\xrightarrow{Fourier}$ $\rho_{calc}^{Fourier}$ Completely model biased

2) F_{obs}, f^{calc} $\xrightarrow{Fourier}$ $\rho_{obs}^{Fourier}$

3) $F_{obs} - F_{calc}$, f^{calc} $\xrightarrow{Fourier}$ $\rho_{diff}^{Fourier}$ Least model biased

MODELED AND EXPERIMENTAL FOURIER MAPS

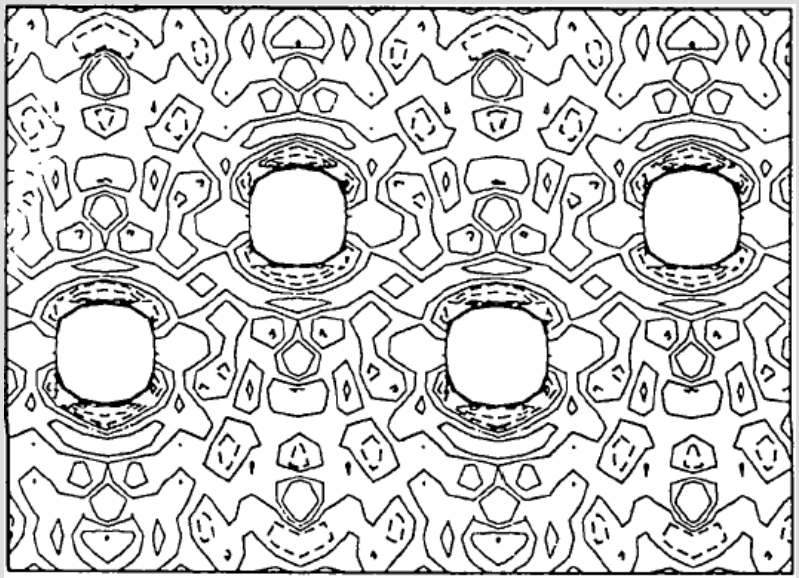

Fourier map of experimental data of silicon in the (110) plane obtained by a Fourier synthesis of the structure factors for which $\sin\theta/\lambda = 0.86$ Å^{-1}. Contour intervals are at 0.1*e*/Å^3 (cutoff level 1.6*e*/Å^3).

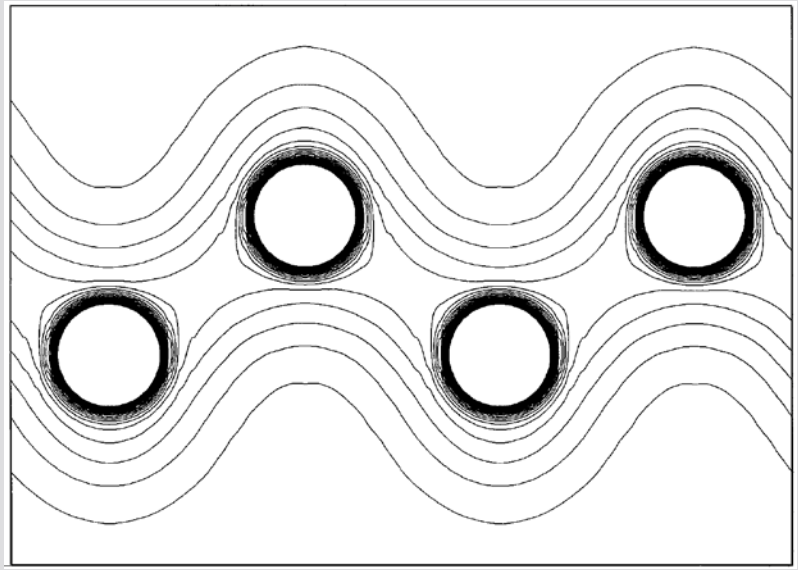

Fourier map of model data of silicon in the (110) plane obtained by a Fourier synthesis of the structure factors for which $\sin\theta/\lambda = 5.5$ Å^{-1}. Contour intervals are at 0.1*e*/Å^3 (cutoff level 2.5*e*/Å^3).

de Vries, R.Y.; Briels, W.J.; Feil, D. // PHYS. REV. LETT. 1996. 77. 1719-1722.

Sakata, M.; Sato, M. // ACTA CRYST. 1990. V. A46. P. 263-270.

DETERMINATION OF THE ELECTRON-DENSITY DISTRIBUTION FOURIER MAP ↔ MEM MAP

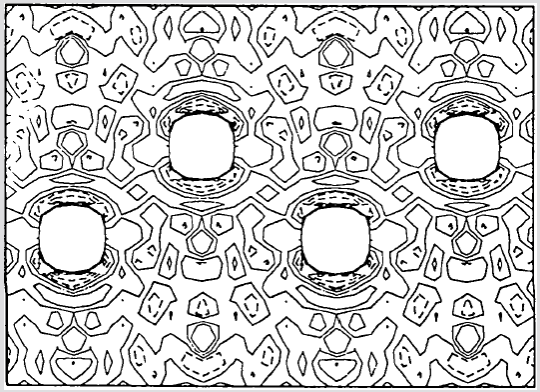

- a perfect Fourier map would require a complete set of structure factors up to at least sin $\theta/\lambda = 5.0\ A^{-1}$
- allows the location of missing atoms
- may show strong peaks that do not correspond to atoms

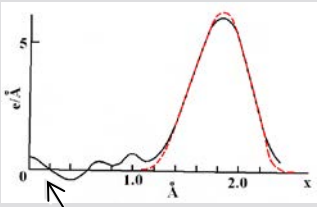

series termination errors

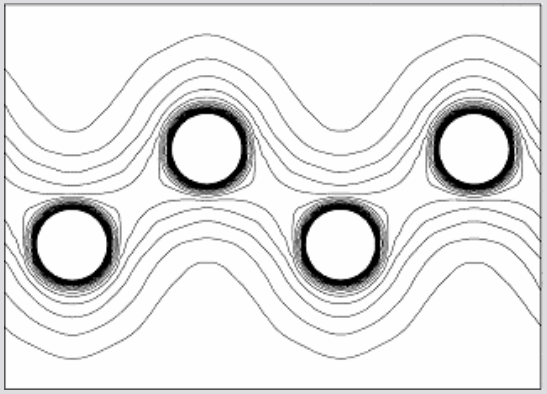

- allows to incorporate prior information
- does not involve numerical Fourier transform => no series termination errors.
- can successfully work with structure factors from powder data with a resolution of sin $\theta/\lambda \approx 0.6\ °A^{-1}$.
- allows the location of missing atoms
- peaks that do not correspond to atoms in the current model always have the density of the noise level

MEM CALCULATIONS WITH FLAT PRIOR AND DIFFERENT RESOLUTION SINθ/λ

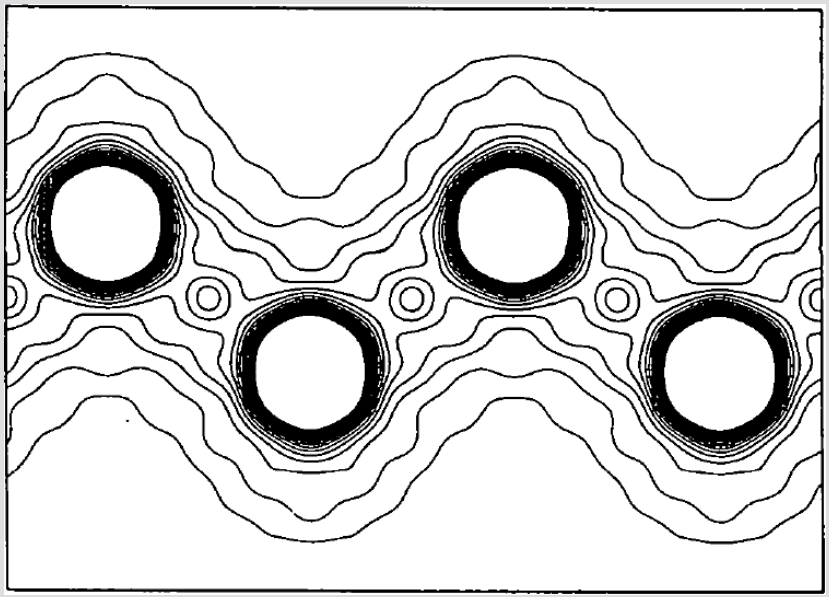

MEM map of experimental data of silicon in the (110) plane obtained using the <u>flat prior</u> and the calculated structure factors for which $\sin\theta/\lambda$ = 0.86 Å^{-1}. Contour intervals are at 0.1*e*/Å^3 (cutoff level 2.5*e*/Å^3).

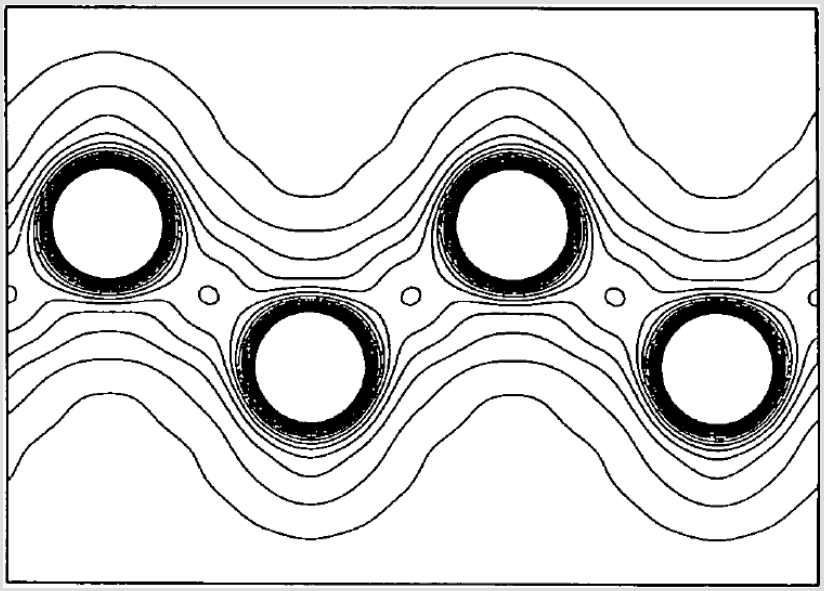

Same as left side but $\sin\theta/\lambda$ = 1.04 Å^{-1}.
➔ just 2 more Bragg reflections !!!

Sakata, M.; Sato, M. // ACTA CRYST. 1996. V. A52. P. 287-290.

PRIOR DENSITY IN MEM CALCULATIONS

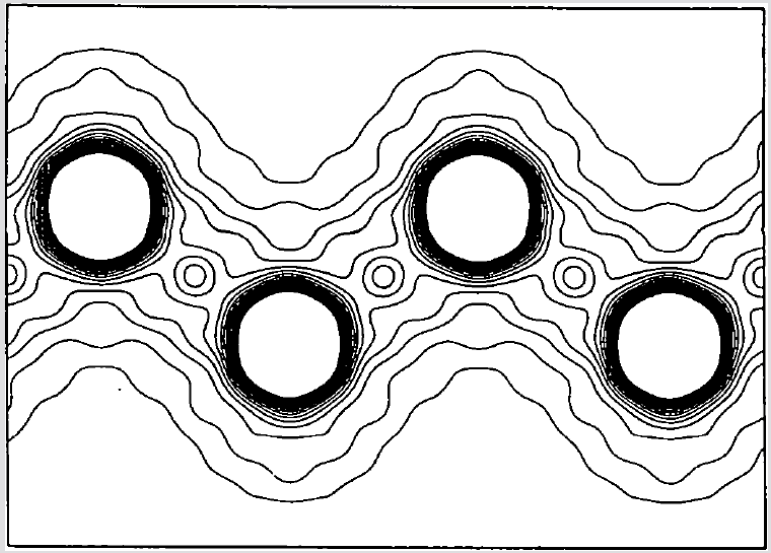

MEM map of experimental data of silicon in the (110) plane obtained using the flat prior and the calculated structure factors for which sinq/l = 0.86 $Å^{-1}$. Contour intervals are at 0.1*e*/$Å^3$ (cutoff level 2.5*e*/$Å^3$).

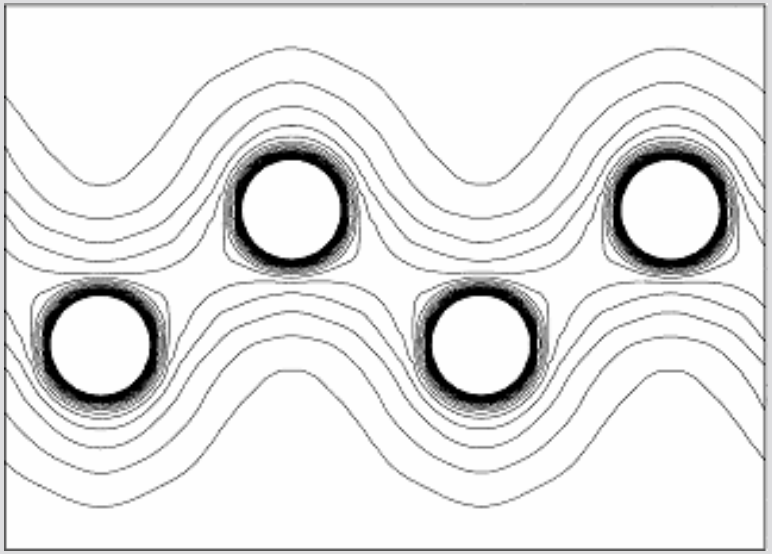

Same as left side but using the procrystal density (ISAM).

de Vries, R.Y.; Briels, W.J.; Feil, D. // PHYS. REV. LETT. 1996. 77. 1719-1722.

ELECTRON-DENSITY DISTRIBUTION IN APATITES WITH INTERCALATED METAL ATOMS

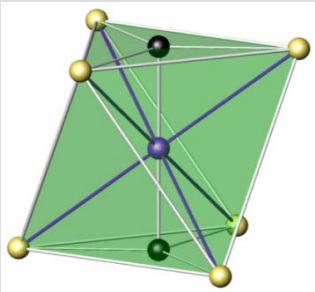

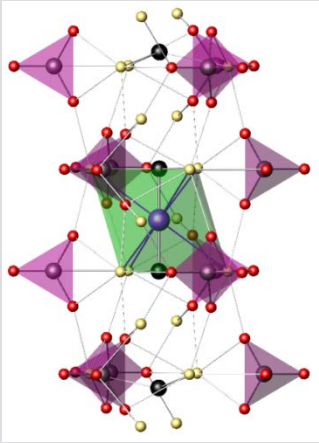

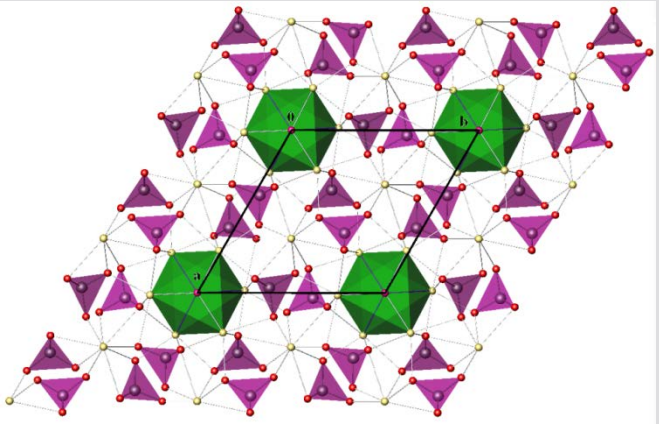

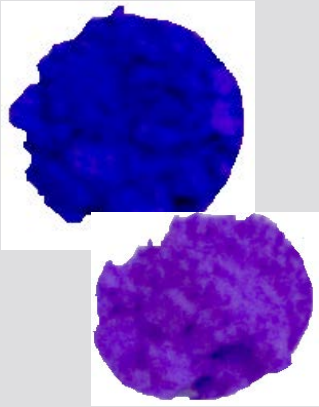

Molecular formula	$Sr_5(PO_4)_3Cu_xO_{2x}(OH)_{1-2x}$
Space group	$P6_3/m$ (176)
Z	2
a / Å	9.77
c / Å	7.28

Karpov, A.S.; Nuss, J.; Jansen, M.; Kazin, P.E.; Tretyakov, Yu.D. // Solid State Science. 2003. V.5. P.1277-1283.

Kazin, P.E.; Karpov, A.S.; Jansen, M.; Nuss, J.; Tretyakov, Yu.D. // Z. Anorg. Allg. Chem. 2003. V. 629. P. 344-352.

Kazin, P.E.; Gazizova, O.R.; Karpov, A.S.; Jansen, M.; Tretyakov, Yu.D. // Solid State Science. 2007. V. 9. P. 82-87.

LOCALIZATION OF MISSING ATOMS IN THE INCOMPLETE CRYSTAL STRUCTURE OF APATITE $Ca_5(PO_4)_3CU_{0.05}O_{0.5}H_{0.45-\delta}F_{0.5}$

$\rho^{Fourier}_{calc}$

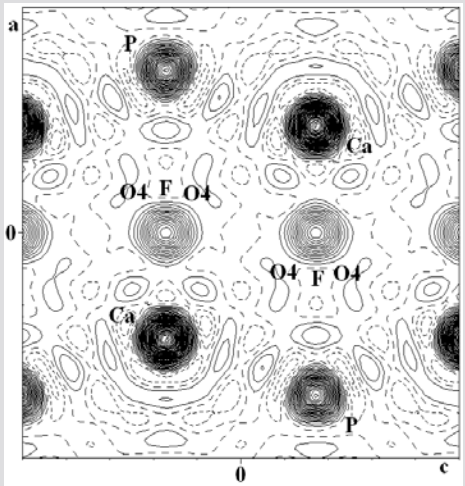

$\rho^{Fourier}_{obs}$

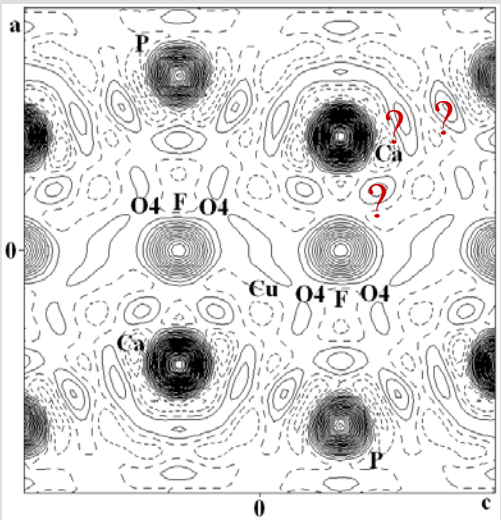

$\rho^{Fourier}_{diff}$

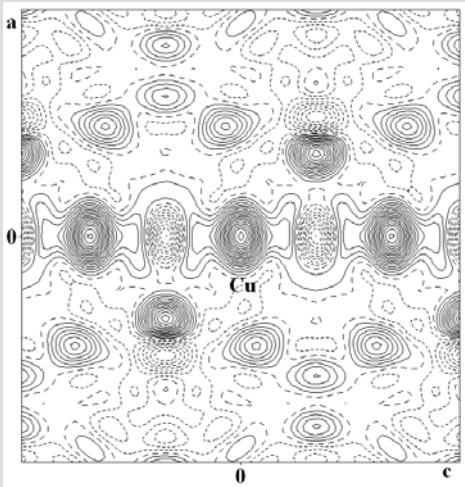

There is no Fourier map that allows to locate the Cu atoms unambiguously

X-ray laboratory data
$\sin\theta/\lambda = 0.55$ Å^{-1}

Contour levels: from 1 to 50 e/Å^3, step 1 e/Å^3

LOCALIZATION OF MISSING ATOMS IN THE INCOMPLETE CRYSTAL STRUCTURE OF APATITE $Ca_5(PO_4)_3CU_{0.05}O_{0.5}H_{0.45-\delta}F_{0.5}$

ρ_{calc}^{MEM}

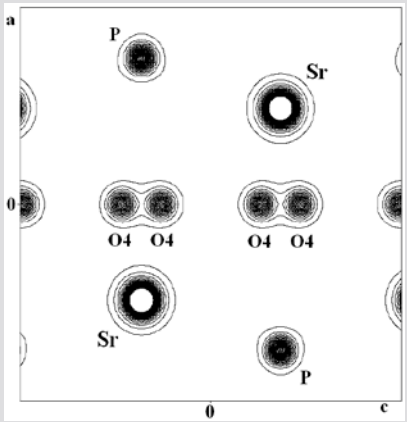

ρ_{obs}^{MEM}

procrystal density

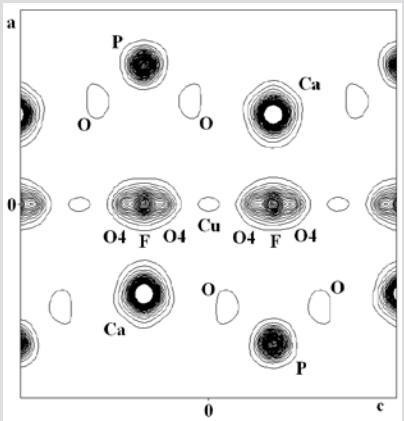

ρ_{obs}^{MEM}

flat prior

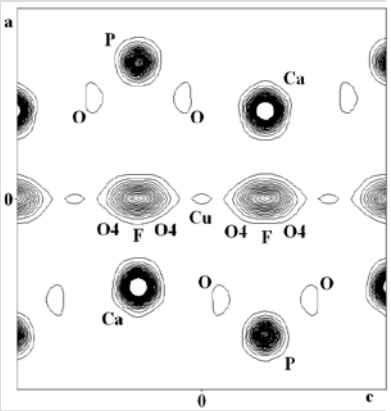

ρ_{obs+G}^{MEM}

procrystal density

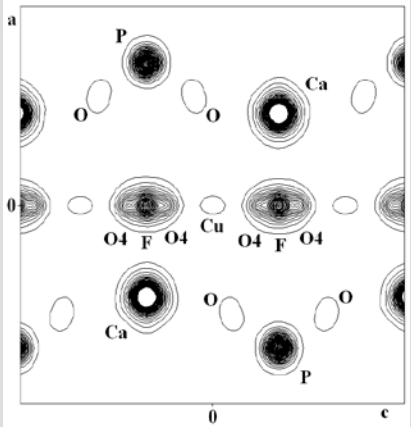

$\rho_{LeBail+G}^{MEM}$

procrystal density

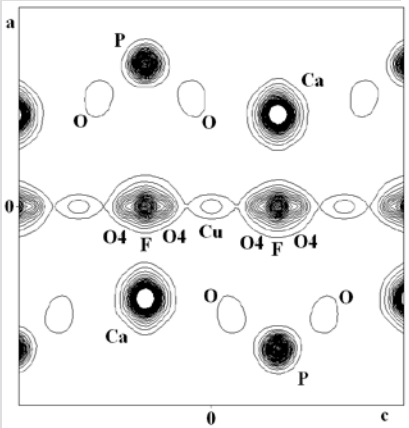

X-ray laboratory data
$\sin\theta/\lambda = 0.55$ Å^{-1}

Contour levels: from 1 to 50 e/Å^3, step 1 e/Å^3

DETERMINATION OF THE EDD OF INTERCALATED COPPER ATOMS USING MEM MAPS

1

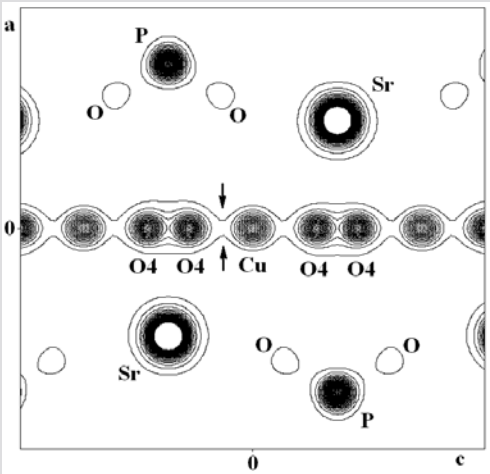

2

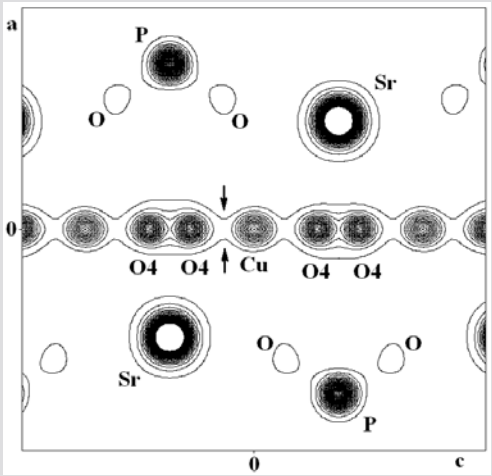

3

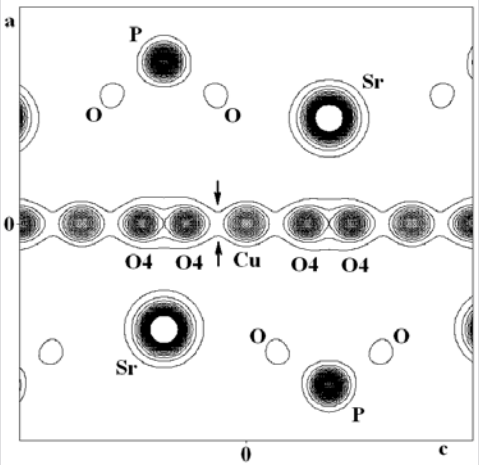

4

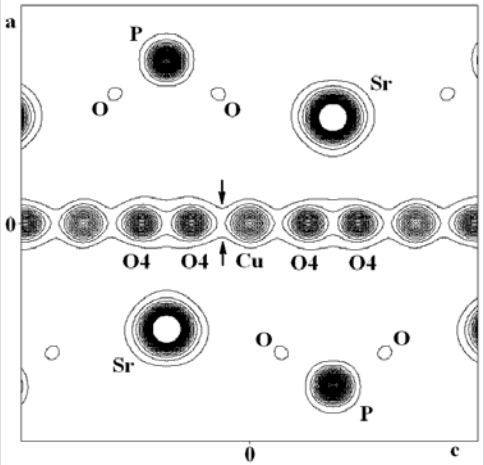

Contour levels: from 1 to 50 e/Å^3, step 1 e/Å^3

X-ray laboratory data
$\sin\theta/\lambda = 0.55$ Å^{-1}

All compounds have the same content of Cu = 0.1, but different amount of peroxide

1 – 1.9 % of peroxide
2 – 3 % of peroxide
3 – 15 % of peroxide
4 – >15 % of peroxide

The distribution of the electron density is distorted due to the increasing content of peroxide molecules

DETERMINATION OF THE EDD OF INTERCALATED COPPER ATOMS USING MEM MAPS

1

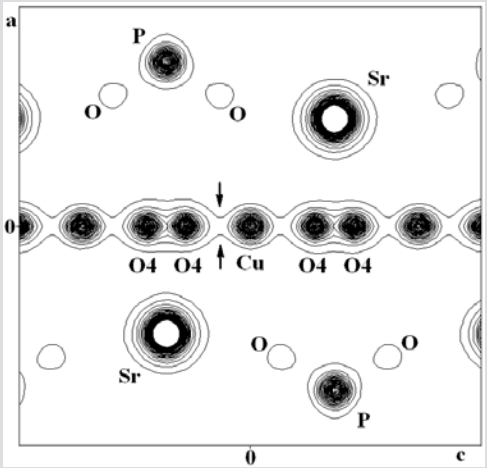

2

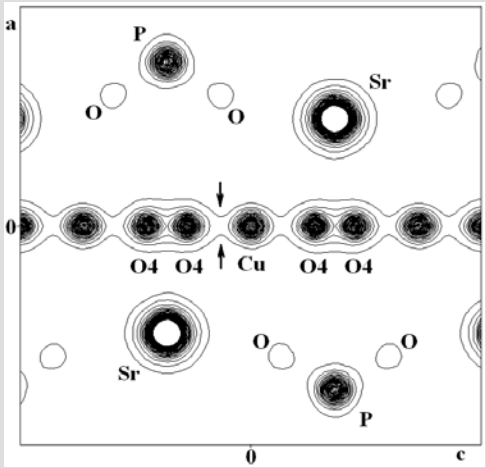

3

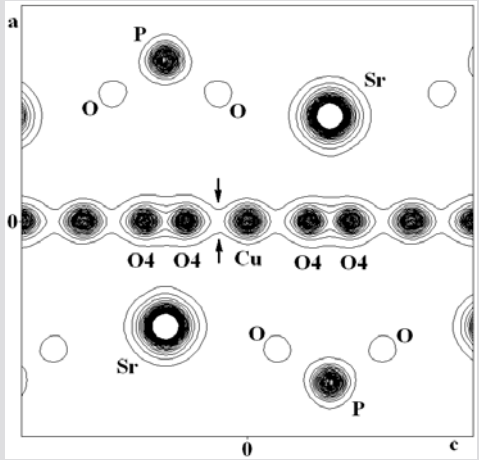

4

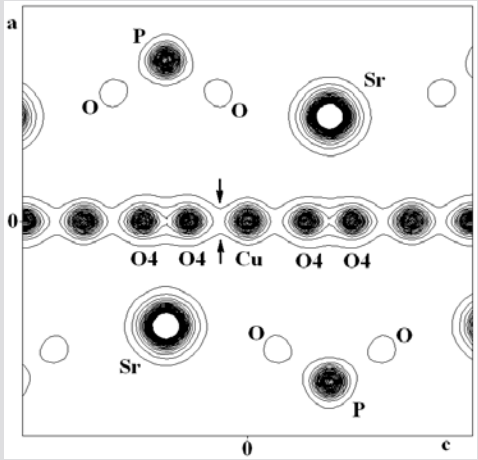

Contour levels: from 1 to 50 e/Å^3, step 1 e/Å^3

Synchrotron data $\sin\theta/\lambda$ = 0.55 Å^{-1}

All compounds have the same content of Cu = 0.1, but different amount of peroxide

1 – 1.9 % of peroxide
2 – 3 % of peroxide
3 – 15 % of peroxide
4 – >15 % of peroxide

The distribution of the electron density is distorted due to the increasing content of peroxide molecules

MEM MAP FROM POWDER
↔
EDD FROM SINGLE CRYSTAL

□-$RbAg_4I_5$ ionic conductor $P4_132$ *a*=11.2500 Å

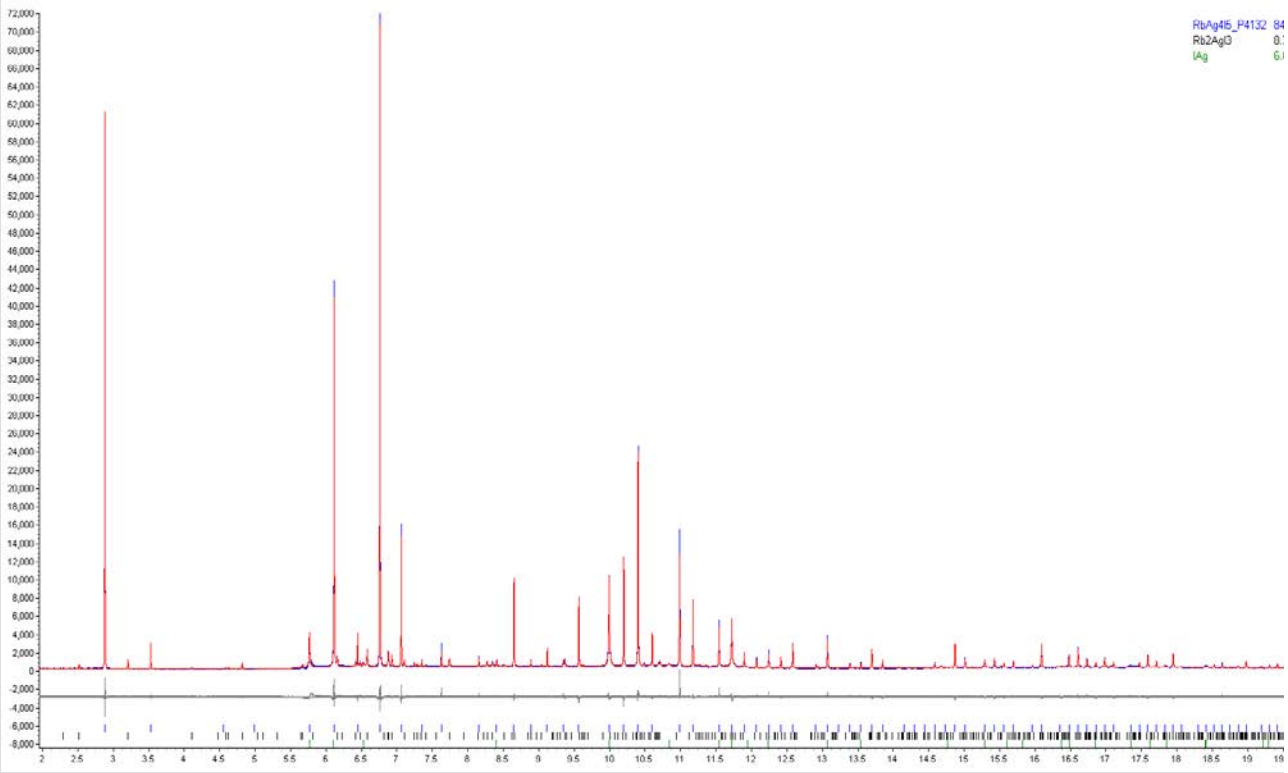

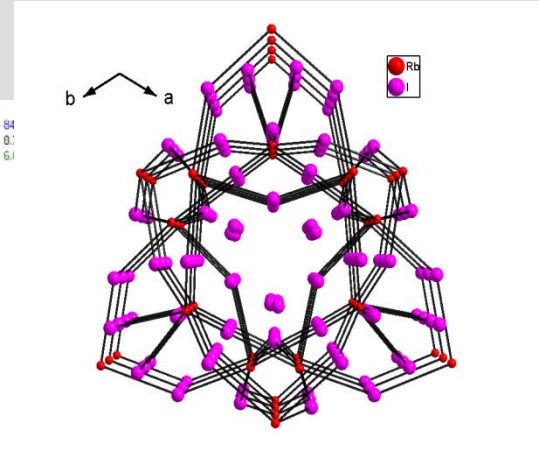

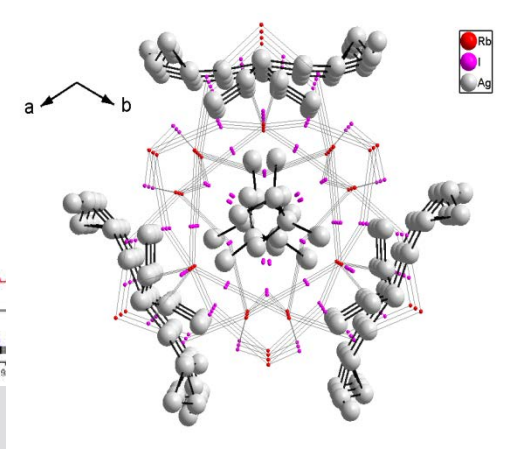

Parameters of the Rietveld refinement:
Rwp = 7.13%, Rp = 5.23%, R_I = 3.10%, GooF = 1.64

SINGLE CRYSTAL EDD
↔ RIETVELD FROM POWDER
↔ MEM MAP FROM POWDER

Ag1

Ag2

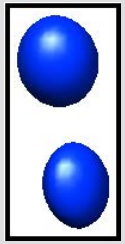

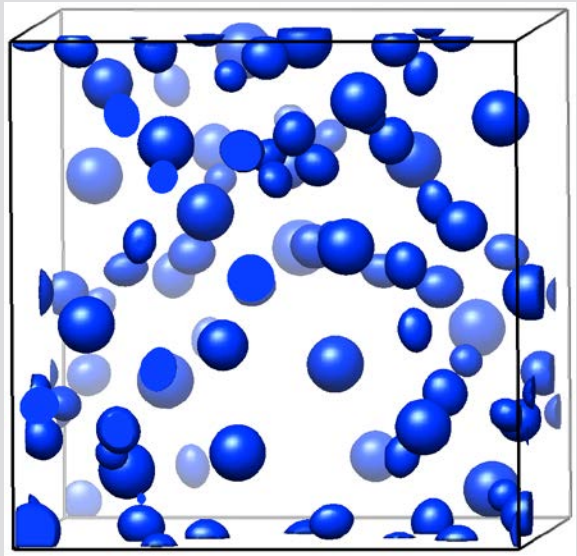

single crystal EDD

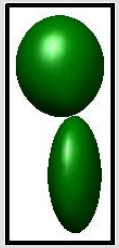

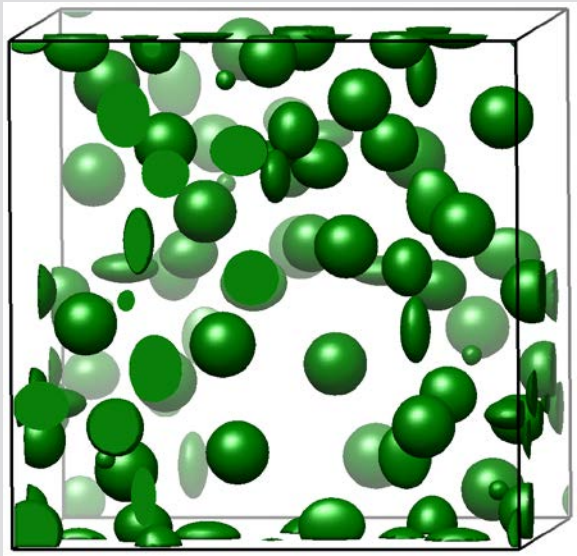

anisotropic ADPs from Rietveld refinement

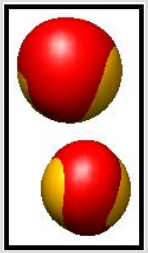

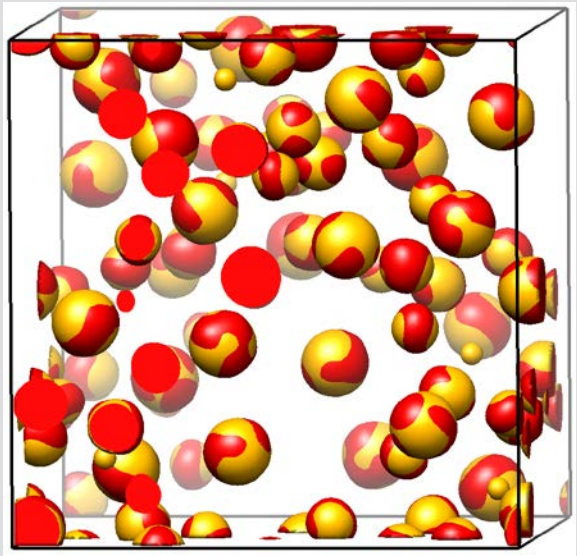

red – MEM reconstructed ED

yellow – ISAM

THE HIGH TEMPERATURE PHASES OF RUBIDIUM OXALATE BY IN SITU POWDER DIFFRACTION

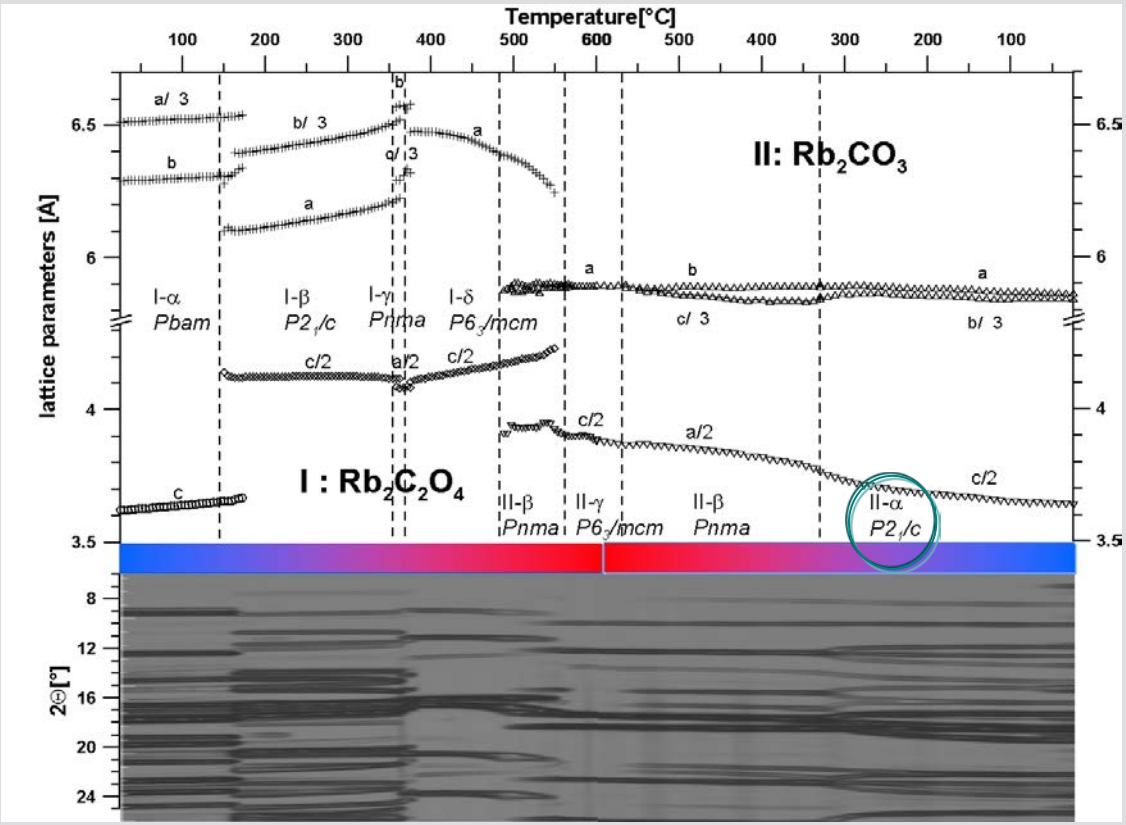

T: 25°-450°-25°

200 scans in 3½ hrs

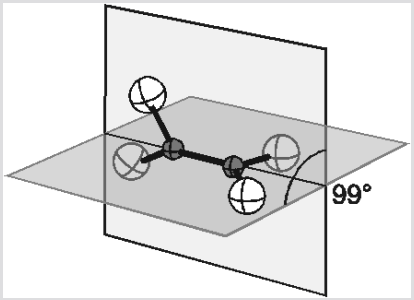

R. E. Dinnebier, S. Vensky, M. Jansen, and J. Hanson, Crystal Structures of and Topological Aspects on the High Temperature Phases and the Decomposition Products of the Alkali Oxalates $M_2[C_2O_4]$, M=(K, Rb,Cs), *2005, Chemistry, a European Journal, 11, 1119 – 1129.*

A. Samy, R. E. Dinnebier, S. van Smaalen, and M. Jansen, The Maximum Entropy Method and Charge Flipping, a powerful combination to visualize the true nature of structural disorder from *in situ* X-ray powder diffraction data. *(2010) Acta Cryt. B.*

THE HIGH TEMPERATURE PHASES AND DECOMPOSITION PRODUCTS OF RUBIDIUM OXALATE

$Rb_2C_2O_4$

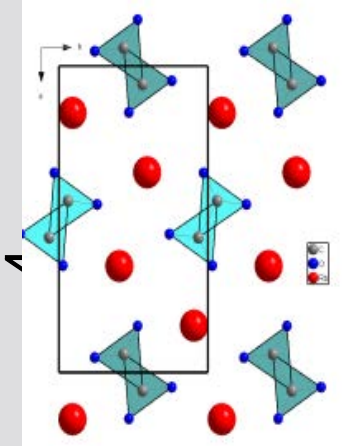

Pbam →

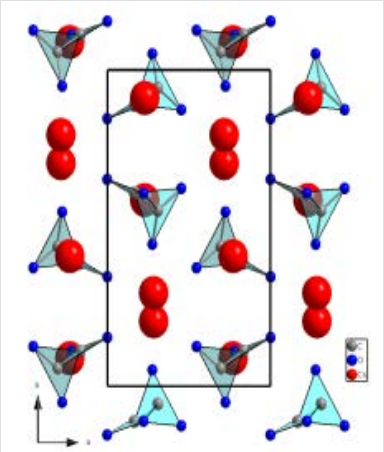

$P21_1/c$ ↔

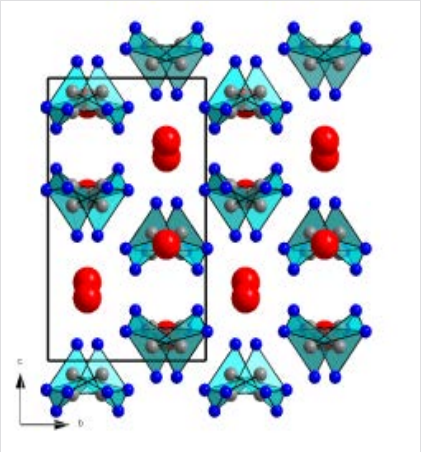

Pnma ↔

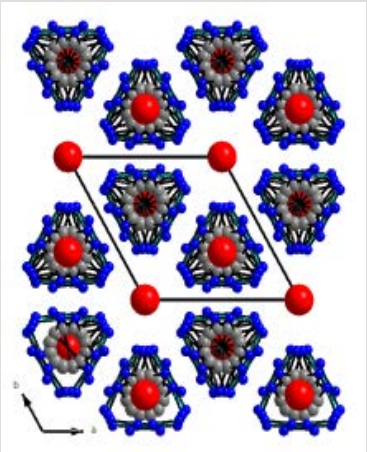

$P6_3/mmc$

Rb_2CO_3

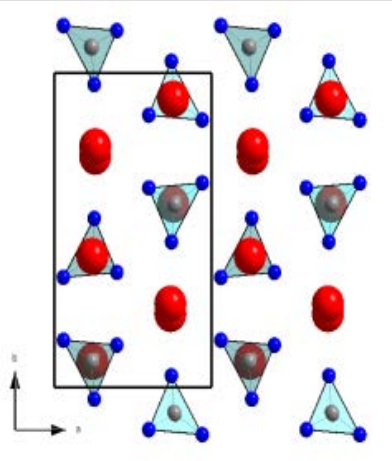

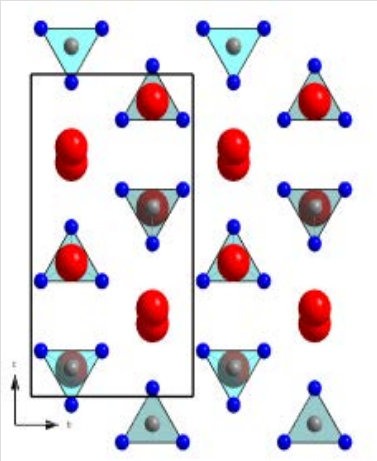

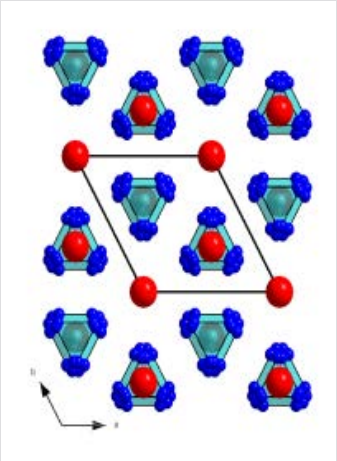

RESULTS OF MEM-CALCULATIONS BASED ON MODEL-RIETVELD-REFINEMENT

	Prior: IAM	MEM-Fcalc:	MEM-Fobs:	MEM-Fobs-G-constr.
	Strong-biased	All F biased	F_{obs} partially biased	Less biased
δ-$K_2C_2O_4$ (*Pbam*) ordered T = 295 K	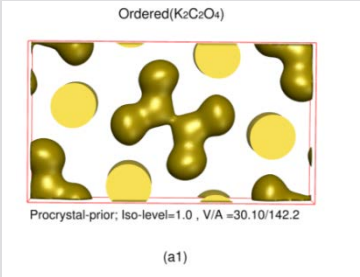	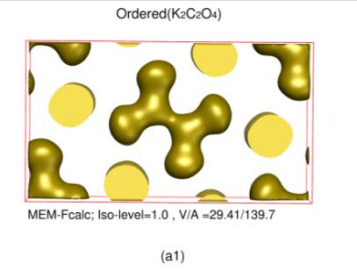	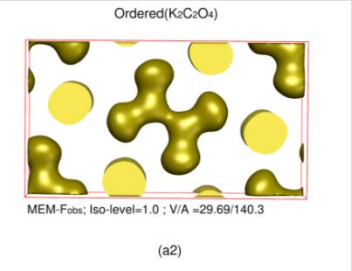	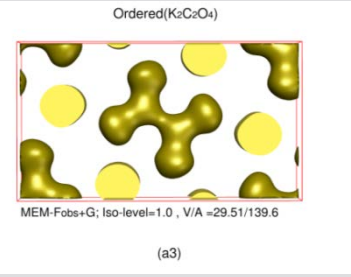
α-$Rb_2C_2O_4$ (*P6$_3$/mmc*) disordered T = 683 K	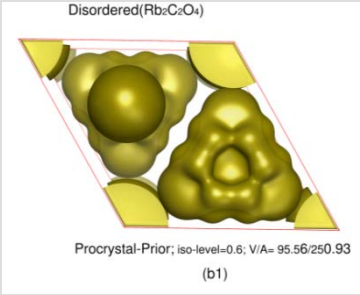	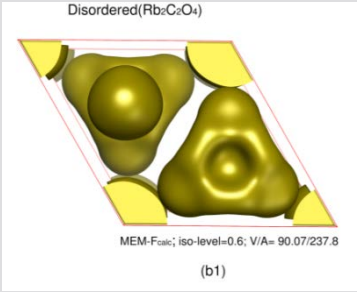	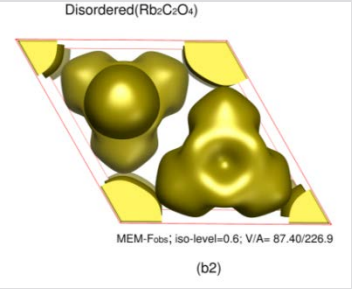	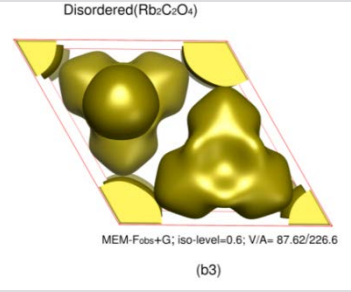
α-Rb_2CO_3 (*P6$_3$/mmc*) disordered T = 860 K	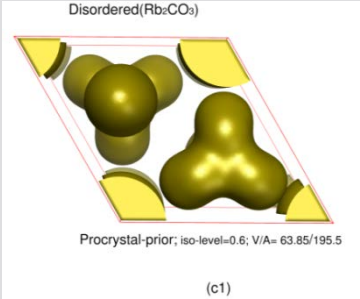	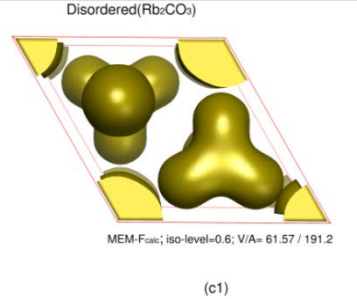	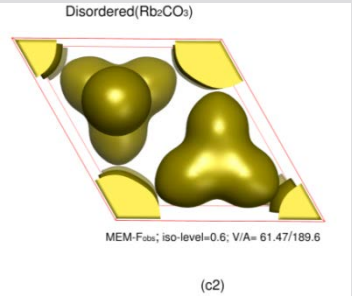	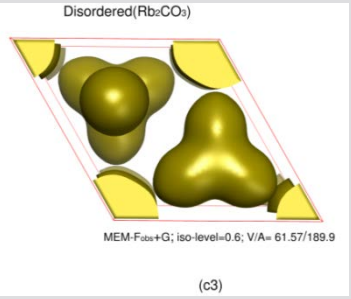

CHARGE FLIPPING + MEM

$$F_{LeBail}+G,\ f^{Rietveld} \xrightarrow{MEM} \rho^{MEM}_{LeBail+G}$$

$$F_{LeBail}+G,\ f^{Charge\ Flipping} \xrightarrow{MEM} \rho^{MEM}_{LeBail+G}$$

1) structure-factor amplitudes are obtained by Le Bail fit
2) structure-factor phases are determined by charge flipping with histogram matching

Completely *ab-initio* electron-density distribution!!!

Ali Samy, Robert E. Dinnebier, Sander van Smaalen, Martin Jansen // ACTA CRYST. 2010. B 66, 184–195

CHARGE FLIPPING + MEM

Distribution of the electron densities from Rietveld refinement:

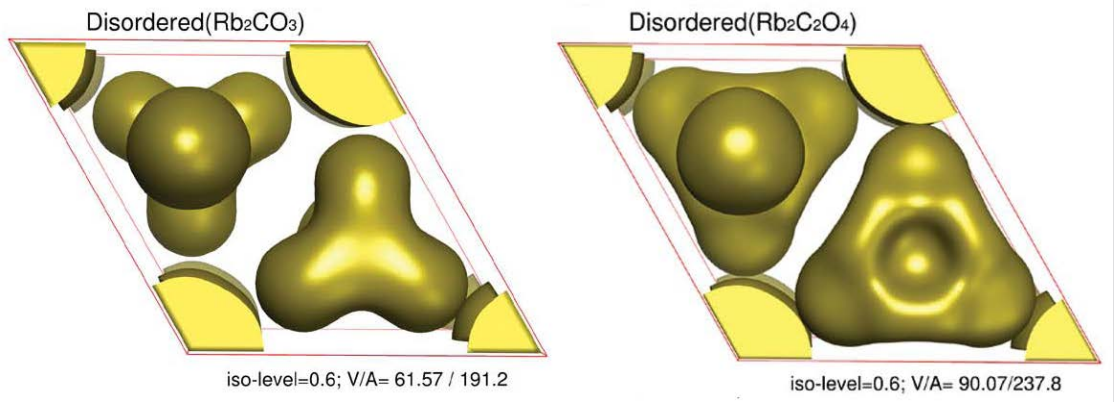

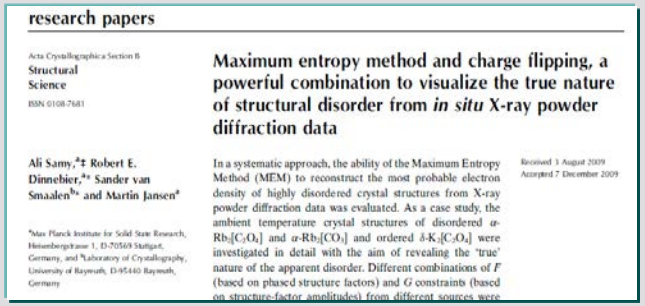

research papers

Acta Crystallographica Section B
Structural Science
ISSN 0108-7681

Maximum entropy method and charge flipping, a powerful combination to visualize the true nature of structural disorder from *in situ* X-ray powder diffraction data

Ali Samy,[a]‡ Robert E. Dinnebier,[a]* Sander van Smaalen[b]* and Martin Jansen[a]

[a]Max Planck Institute for Solid State Research, Heisenbergstrasse 1, D-70569 Stuttgart, Germany, and [b]Laboratory of Crystallography, University of Bayreuth, D-95440 Bayreuth, Germany

In a systematic approach, the ability of the Maximum Entropy Method (MEM) to reconstruct the most probable electron density of highly disordered crystal structures from X-ray powder diffraction data was evaluated. As a case study, the ambient temperature crystal structures of disordered α-$Rb_2[C_2O_4]$ and α-$Rb_2[CO_3]$ and ordered δ-$K_2[C_2O_4]$ were investigated in detail with the aim of revealing the 'true' nature of the apparent disorder. Different combinations of *F* (based on phased structure factors) and *G* constraints (based on structure-factor amplitudes) from different sources were

Received 3 August 2009
Accepted 7 December 2009

Distribution of the electron densities from Charge Flipping + MEM:

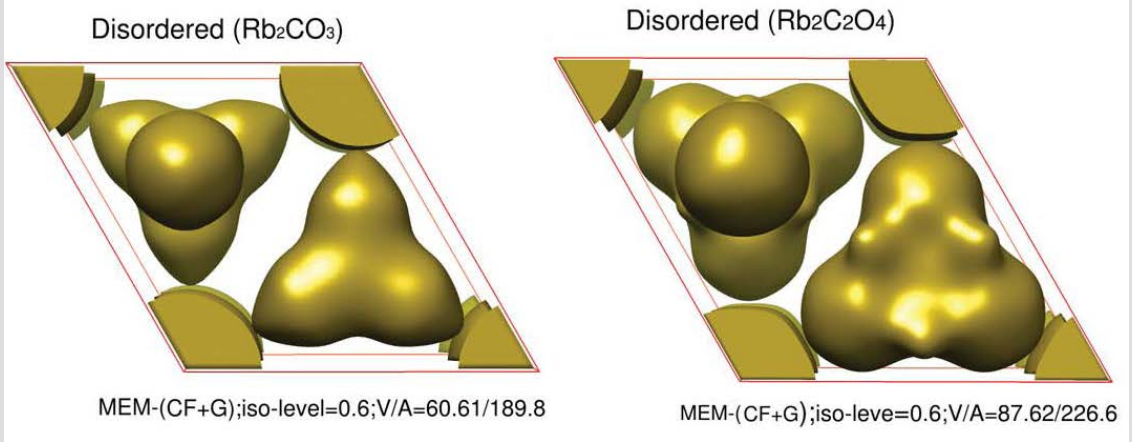

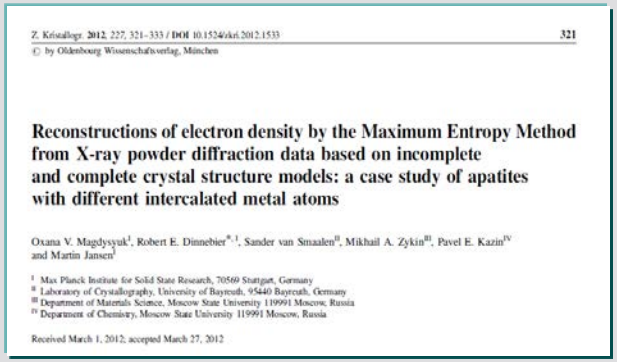

Z. Kristallogr. 2012, 227, 321–333 / DOI 10.1524/zkri.2012.1533 321
© by Oldenbourg Wissenschaftsverlag, München

Reconstructions of electron density by the Maximum Entropy Method from X-ray powder diffraction data based on incomplete and complete crystal structure models: a case study of apatites with different intercalated metal atoms

Oxana V. Magdysyuk[I], Robert E. Dinnebier[*, I], Sander van Smaalen[II], Mikhail A. Zykin[III], Pavel E. Kazin[IV] and Martin Jansen[I]

[I] Max Planck Institute for Solid State Research, 70569 Stuttgart, Germany
[II] Laboratory of Crystallography, University of Bayreuth, 95440 Bayreuth, Germany
[III] Department of Materials Science, Moscow State University 119991 Moscow, Russia
[IV] Department of Chemistry, Moscow State University 119991 Moscow, Russia

Received March 1, 2012; accepted March 27, 2012

Ali Samy, Robert E. Dinnebier, Sander van Smaalen, Martin Jansen // ACTA CRYST. 2010. B 66, 184–195

SOME CONCLUSIONS

- New detectors and better X-ray sources allow to fully track structural changes in the sub-second regime.
- New software for data reduction (e.g. Powder3D-IP), visualization (e.g. Powder-3D) and sequential/parametric WPPF refinement (e.g. Topas 5.0) allow to handle (semi-)automatically huge numbers of powder patterns.
- Rietveld refinement and MEM allow for the investigation of advanced structural features (inaccessible to Fourier analysis) like : disorder, diffusion pathways in ionic conductors or distribution of electron density.
- The MEM is very well suited to locate even small anmounts of intercalated atoms in crystal structures from XRPD
- Complex structure determination from XRPD by the combination of CF and MEM is possible.

ACKNOWLEDGMENT

The diffraction group of the MPI-FKF

Robert Dinnebier
(Head of group)

Frank Adams
(Engineer)

Christine Stefani
(CTA)

Martin Etter
(Ph.D student)

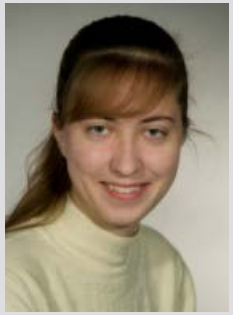

Oksana Magdysyuk
(Ph.D student)

Melanie Müller
(Ph.D student)

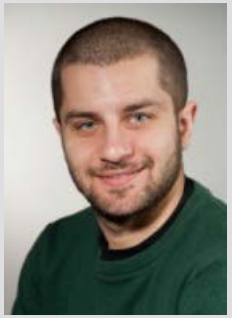

Tomce Runcevski
(Ph.D student)

External collaborators

Ivan Halasz (Zagreb university), Tomislav Friščić (McGill),Peter Stephens (SUNY at Stony Brook), John Hanson (NSLS), Sander van Smaalen (Bayreuth), Andy Fitch (ESRF),Branton Campbell (BYU), Andreas Leineweber (MPI-IS), Michael Hirscher (IS-MPG), Pavel Kazin (Moscow)…

Facilities & Beamline staff

NSLS, FRM-II, ESRF, Diamond, Petra III

SOME HOUSE ADVERTISING…